HPLC-UV QUANTITATION OF FOLATE SYNTHESIZED BY RICKETTSIA ENDOSYMBIONT IXODES PACIFICUS (REIP)

By

Junyan Chen

A Thesis Presented to

The Faculty of Humboldt State University

In Partial Fulfillment of the Requirements for the Degree

Master of Science in Biology

Committee Membership

Dr. Jianmin Zhong, Committee Chair

Dr. David S. Baston, Committee Member

Dr. Jenny Cappuccio, Committee Member

Dr. Jacob Varkey, Committee Member

Dr. Erik Jules, Program Graduate Coordinator

December 2017

ABSTRACT

HPLC-UV QUANTITATION OF FOLATE SYNTHESIZED BY RICKETTSIA ENDOSYMBIONT IXODES PACIFICUS (REIP)

Junyan Chen

Ticks are the most important vector of many infectious diseases in the United States. Understanding the nature of the relationship between *Rickettsia* endosymbiont *Ixodes pacificus* (REIP) and *Exudes pacificus* will help develop strategies for the control of tick-borne diseases, such as Lyme disease, and Rocky Mountain spotted fever. Folate, also known as vitamin B9, is a necessary vitamin for tick survival, and plays a central role in one-carbon metabolism in cells. Folate exist as a large family of structurally related forms that transfer one-carbon groups among biomolecules that are important to cell growth, differentiation, and survival. In Dr. Zheng's lab, REIP were cultured in *Ixodes scapularis* embryonic tick cell line ISE6. Previous research has shown that REIP in *Ixodes pacificus* carries all five *de novo* folate biosynthesis genes. Folate biosynthesis mRNAs were detected and all recombinant rickettsial folate proteins were overexpressed. To determine whether REIP synthesize folate, we sought to measure the folate concentration in REIP using HPLC-UV quantification with a Diamond Hydride™ liquid chromatography column. 5-methyltetrahydrofolate (5-MTHF), the active circulating form of folate in bacteria was detected. The averaged folate level in the REIP-infected ISE6 pellet is 0.2514 mg/L/10^6 cells, which is 5-fold higher than the pellet sample from uninfected

ISE6 pellet sample. For the REIP-infected ISE6 supernatant sample, the measured concentration is 0.0029 mg/L/10^6 cells. Statistical analysis using t-test determined there is a statistical significance (p=0.05) in the folate concentrations between REIP-ISE6 pellets and ISE6 pellets; REIP-ISE6 pellet and REIP-ISE6 supernatant. However, more analysis is required to confirm the identity of the 5-MTHF peak before we draw the conclusion that REIP can synthesize folate. Additionally, we sought to knockout the *folA* gene in REIP to confirm folate is synthesized by REIP. We used the TargeTron system to construct the knockout, however, no successful mutant *Rickettsia* were obtained so far. Furthermore, because REIP classification was not determined yet, we sought to construct a phylogenetic tree of the species. Surprisingly, we identified that REIP was a new subspecies with the following classification *Rickettsia monacensis* subsp. *pacifica* subsp nov. To our knowledge, this is the first report of the present of *R. monacensis* in *I. pacificus* in North America.

ACKNOWLEDGEMENTS

First, I would like to thank my advisor Dr. Jianmin Zhong. He is very patient with me; without his encourage and help, I don't think I can graduate in two and half years. Then I would also like to thank Dr. Maria Matyska-Pesek, Dr. Joseph Pesek, Joshua Topete, Ichi Watanabe, for their kindness and for allowing me to use their HPLC instrument to detect the folate concentration in my samples. I also would like to thank my undergraduate researchers: Erick Morales, Oliver Gonzalez Bobadilla, Makalani Norman, Joselin Jaimes, Guillermo Soto, Cristian Nazarek, Kylie Walker; my labmates Kristine Loew, Maryam Tariq Alowaysi, Monique LaCourse and Jimmy Bodnar for contributing to the project. In addition, I would also like to thank Susan Wright, Marty Reed, and Lewis McCrigler for their help in machine support. What's more, I would like to thank Dr. David Baston (CNRS Core Research Facility, HSU), Dr. Jenny Cappuccio, and Dr. Jacob Varkey from my thesis committee for their comments and help. Finally, yet importantly, I would like to thank my family members for supporting me for the last two and half years to complete my thesis project.

TABLE OF CONTENTS

LIST OF TABLES

LIST OF FIGURES

LIST OF APPENDICES

INTRODUCTION

Background Information

Vector-borne diseases are common human illnesses. They are normally caused by parasites, viruses and bacteria transmitted by the bite of infected arthropod species, such as mosquitoes, ticks, sandflies, and blackflies (Confalonieri, 2007; Brites-Neto, 2015). Ticks are the most important vector of arthropod-borne infections and transmit a wide variety of zoonotic pathogens (Hornok, 2017; Polo, 2017). Tick-borne rickettsial diseases (TBRD) continue to cause severe illness and death among human beings. In the United States, some TBRD are quite common. For example, Rocky Mountain spotted fever (RMSF) and Lyme borreliosis. Researchers found that these TBRD could be easily cured with antibiotics at their early clinical course; however, the greatest challenge to clinicians is their accurate diagnosis early on. Because early signs and symptoms of these illnesses are notoriously nonspecific or mimic those of benign viral illnesses, and the lack of a gold standard for diagnosis makes producing accurate statistics difficult (Alice et al, 2006; Perronne, 2014). In trying to treat patients with TBRD, researchers realized that TBRD is caused by bacteria. One of the pathogens that causes TBRD is Rickettsia species, named after Howard Taylor Ricketts (1871-1910), who studied Rocky Mountain spotted fever in the Bitterroot Valley of Montana and unfortunately died of typhus when studying that disease. Investigations into the endosymbiotic behavior of non-pathogenic species may prove more productive for the development of more effective treatment

methods, such as more specific anti-folate drugs, or the establishment of more efficient eradication methods, such as creation of transgenic ticks, which would decrease the incidence of all tick-borne diseases.

Bacterial Symbiosis

The etymology of the word “symbiosis” is Greek words ‘together’ and ‘living’, which describes a partnership of different organisms living together. In a symbiotic relationship, “host” and “symbiont” are using to describe the larger partner and smaller partner, individually. If one of the partner cannot live individually, the relationship is called “obligate”; otherwise, it is termed “facultative”. What’s more, the symbiosis can be harmful, this is termed as parasitic; or can be beneficial, which is termed mutualistic (Rymaszewska, 2007). When a symbiont lives within a host either intracellular or extracellular, it is referred to as an endosymbiont (Silva, 2012), which theory was first proposed in 1905 by the Russian botanist Konstantin Mereschkowsky (Mereschkowsky, 1905). Konstantin found the division of chloroplasts in green plants close related with free-living cyanobacteria. Later in 1967, Lynn Sagan (later Lynn Margulis) advanced and substantiated this symbiont theory with microbiological evidence (Margulis, 1967).

Primary and Secondary Endosymbiont of Insects

On earth, insects occupied more than 90% of known animal species, dominating a variety of terrestrial habitats (Douglas, 2014). Even though it has been long known that insects are symbiosis with bacteria, but only in the last few decades researchers start to pay attention on the symbiont relationship between insects and bacteria. Traditionally, symbiont bacteria are separate into two main groups: obligate (primary) symbionts and facultative (secondary) symbionts (Baumann, 2005). Obligate symbionts are mutualists that tend to have a nutritional function and typically occur in insects that feed on unbalanced diets such as plant saps or cellulose (Moya, 2008). For example, *Buchnera* widely distribute in most species of aphid can synthesis amino acids and other compounds. Those nutrients are known lack in aphid's phloem diet (Douglas, 2006). Another example bacteria *Wigglesworthia*, feeds on vertebrate blood performs a similar function for tsetse flies (*Glossinia*) (Aksoy, 1995; Moran, 2008).

Beside the obligate symbionts, some bacteria in insects are facultative (secondary) symbionts. Unlike obligate symbiont bacteria, they are not essential for normal host growth and development. However, they are also widely existing in nature. Then it raises the question of how and why such symbionts are maintained. Research found some bacteria can manipulate host production that allow it to spread through the population (Werren, 1997). In most case, the secondary symbiont manipulates reproduction, protecting against natural enemies or facilitating adaptation to changing environments. For example, the insects infected with secondary endosymbiont of the genus *Rickettsiella*, and then the insects' body color can change from red to green in natural

populations to achieve the goal of avoiding the natural predators (Tsuchida, 2010). *Hamiltonella defensa* endosymbionts strongly protects aphids against parasite induced mortality by parasitic wasps (Rothacher, 2016). In addition, gut bacteria symbiont in *Plutella xylostella's* diamondback moth can produce detoxifying enzymes for degradation of insecticides (Indiragandhi, 2007). What's more, researchers also found some bacteria symbionts that can increase arthropods reproductive success (Himler, 2011).

Endosymbiosis Leads to Genome Reduction in Bacteria

Endosymbiosis has played pivotal roles in biological, ecological, and evolutionary diversification. The loss of DNA and genes is widespread in obligate symbionts. Endosymbionts usually have smaller population sizes and a reduced number of essential functions (Wernegreen, 2004; Mccutcheon, 2010). Compared to the free-living bacteria with a size of 4-5 Mb (millions of base pairs) genomes, the genome sizes of these bacterial mutualist genomes are commonly less than 1 Mb. In some extreme case, the genome size of bacteria is reduced to 139 kb (kilobase), which is known as the smallest bacterial genome so far (McClure, 2017). Such severe genome reducing very likely make the bacteria irreversible live dependence with hosts' intracellular environment. Then another question is raised whether these bacteria should be considered as organisms distinct from their host (Douglas, 2014). So far, researchers have noticed endosymbiotic bacteria affect the biology of hosts in a number of ways, although endosymbiosis remains rich with mysteries.

Introduction of *Ixodes pacificus*

Ticks are the primary vector of many important infectious diseases in the United States; they are obligate hematophagous ectoparasites of mammals, birds and reptiles distributed worldwide (Brites-Neto, 2015); they are of enormous medical and veterinary relevance owing to the direct damage they cause to hosts and as vector of a large variety of human and animal pathogens. Ticks are among the most competent and versatile vector of pathogens, and are second only to mosquitoes as vectors of a number of human pathogens (Socolovschi, 2013). Besides carry pathogens, ticks are also known for carry non-pathogenic endosymbiotic bacteria, and those bacteria are transovarially transmitted (Cowdry, 1925; Noda, 1997).

Ixodes pacificus, which belong to order Ixodida, family Ixodidae, genus *Ixodes* species *pacificus,* also known as the western black-legged tick, is broadly distributed along the western coast of the United States. Compared with other arthropods, *Ixodes pacificus* has several unique features, such as a prolonged life span and complex development, hematophagy in all post-embryonic life stages, long feeding periods, and blood digestion within midgut cells (Sonenshine, 1993). All of the above contribute to their success as vectors for bacteria and viruses (Nuttall and Labuda, 2003).

I. pacificus is an ectoparasite, the life cycle of *I. pacificus* consists of four stages: eggs, larva, nymph, and adult (Figure 1) (Taylor, 2012; CDC, 2015). Each active stage seeks a host, feeds, and drops off to develop in the natural environment. The transition from larva to nymph, from nymph to adult, and the ability of female adult to oviposit, is

dependent on the acquisition of a blood meal (Cheng et al., 2013; Williams-Newkirk et al., 2014). The whole life cycle can take up to three years to complete and includes multiple periods of starvation. Under these conditions, the tick enters a dormant state known as diapause, which subjects its bacterial inhabitants to harsher, nutrient limited conditions (Padgett and Lane, 2001).

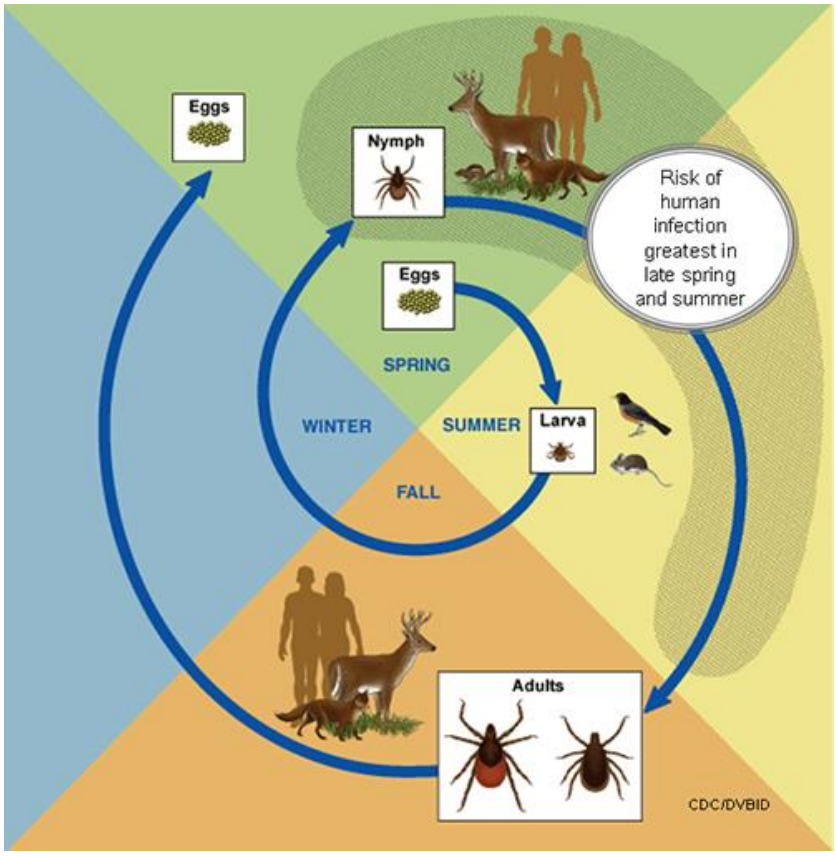

Figure 1. The life cycle of tick. The life cycle of tick includes egg, larva, nymph and adult. At each active stage, they need a blood meal before they can move on to the next stage (CDC, 2015).

I. pacificus increases people's attention since it is a known primary tick vector of the bacteria causing Lyme borreliosis (caused by bacteria *Borrelia burgdorferi*) and

anaplasmosis (caused by bacteria *Anaplasma phagocytophilum*) (Clover and Lane, 1995; Foley, 2008; Piesman, 1999). Each year more than 300,000 cases of Lyme disease are diagnosed in American (Kuehn, 2013). Since 1995, there are at least 15,952 nationally reported anaplasmosis cases, however, the incidence of anaplasmosis has increased 12-fold between 2001 and 2011 (Bakken, 2015). The increasing incidences may have been related with global warming and the expanding range of the tick vector (Dahlgren, 2016). What's more, *I. pacificus* also carries a species of *Ricketssia* currently known as phylotype G021 (Phan, 2011) and is classified as nonpathogenic. Our research is aimed at investigating the natural relationship between endosymbiont *Rickettsia* and *I. pacificus*.

Introduction of *Rickettsia*

Rickettsiae is a diverse collection include the genera *Rickettsiae*, *Ehrlichia*, *Orientia*, and *Coxiella*. All Rickettsiae obligate intracellular gram-negative bacteria. They distribute in a wide range of hosts, like tick, lice, fleas, mite, chigger, and mammal (Walker, 1996).

Rickettsia is a genus of gram-negative, obligate intracellular bacteria with a size range from 0.3 to 2.0 μm. It replicates with binary fission in the cytoplasm of eukaryotic host cells. Consequently, *Rickettsia* must be cultivated in host cells. So far, the common methods culture *Rickettsia* in laboratory using tissue culture, guinea pigs, or embryonated chicken eggs. In addition, Giemsa stain is widely used to observe the *Rickettsia* stains (Ammerman, 2008).

Culture *Rickettsia* in Tick Cell Line

As mentioned above, *Rickettsia* is obligate intercellular bacteria, it cannot reproduce outside the host cells. In our lab, we culture rickettsia in cell line ISE6 derived from *Ixodes scapularis embryos* and cell line IRE11 derived from *Ixodes ricinus* embryos. Both cell lines can grow in mammalian culture media supplemented with mammalian serum, using incubation temperatures between 28ºC to 34ºC. For ISE6 cells, the optimum incubation temperature is 34 ºC. Unlike IRE11 cells, ISE6 cells are able to grow adhering the culture flask surface. Both cell lines divide relatively slowly and can be maintained at high cell density (10^6 to 10^7 cells/mL).

Tick cell lines are cultures derived from tick embryos (eggs), molting larvae or nymphs. Tick cells may grow as monolayers, in suspension, or a mixture of both. Tick cells can survive for months or even years-without subculture; this characteristic is particularly useful for attempted isolation *ex vivo* of slow-growing microorganisms (Bekker et al., 2002).

Tick cell line has been a good tool for study tick-borne pathogens or symbionts due to it allows the microorganisms to propagate without mammalian cell culture (Simser, 2002). All tick cell lines comprise two or more cell types (Yunker, 1987, Bell-Sakyi, 2007). Several types of cells have been described as round, long, bipolar, muscle, epithelial or fibroblast-like (Munderloh, 1994). Since the first *Ixodes* (hard) tick cell lines were established, tick cell lines were not only being used on propagation of tick-borne pathogens, but also used for study tick biology, genomics, proteomics and genetic manipulation (Bell-Sakyi, 2007).

There are two major benefits to studying microorganisms using tick cell lines. First, tick cells are easy and useful for microorganism isolation and molecular characterization (Bell-Sakyi, 2007, 2012). What's more, prolonged culture of some tick-borne pathogens in tick cells facilitates adaptation to mammalian systems (Bekker, 2002; Munderloh, 2004), indicating that tick cell lines are better tools than mammalian cells for microorganisms' isolation. Second, tick cell lines have a great advantage in studying the interaction between tick-borne microorganism and tick *ex vivo*. Tick cell lines can serve as valuable tools to evaluate the pathogens' ability in tick and also help with the study of tick-borne microorganism survival mechanisms in ticks and transmission dynamics in

nature (Bell-Sakyi, 2007). In short, tick cell lines provide wide potential applications for researchers in tick and tick-borne disease research. So far, over 50 tick cell lines have been generated and be developed as tools for ticks and tick-borne pathogens' research (Oliver, 2015).

Rickettsia Classification

The genus *Rickettsia* encompasses a large group of obligate intracellular, gram-negative bacteria that fall under the family Rickettsiaceae, order Rickettsiales, class Alphaproteobacteria, phylum Proteobacteria. The family Rickettsiceae consists of three genera: *Rickettsia*, *Orientia* and *Candidatus Cryptoprodotis*, of which *Rickettsia* and *Orientia* represent two closely related evolutionary lineages that once were considered as belonging to the same genus. To determine the genus of *Rickettsia*, the most normal methods is using sequences of genes coding for citrate synthase (*gltA*) and outer surface proteins (*ompA* and *ompB*) and surface cell antigens (*sca1*, *sca2* and *sca4*) (Merhej, 2014). So far, there are 26 formally recognized species in the genus *Rickettsia*, which can be classified into four groups: the typhus group (*Rickettsia typhi* and *Rickettsia prowazekii*), the spotted fever group (22 *Rickettsia* species, like *Rickettsia aeschlimannii*, *Rickettsia africae, Rickettsia australis, Rickettsia conorii*, *Rickettsia heilongjiangensis, Rickettsia Helvetica, Rickettsia honei, Rickettsia honei* strain marmionii, *Rickettsia japonica, Rickettsia massiliae, Rickettsia monacensis, Rickettsia parkeri, Rickettsia philipii* (364D), *Rickettsia raoultii, Rickettsia rickettsia, Rickettsia sibirica , Rickettsia*

monteiroi , Rickettsia slovaca, Rickettsia tamurae, *Rickettsia argasii, Rickettsia asiatica, Rickettsia peacockii*) *Rickettsia bellii* group, and the *Rickettsia canadensis* group. Although many other isolates exist, they have not been characterized and validated (Socolovschi, et al., 2013).

Intercellular Lifecycle of *Rickettsia*

The members of the order *Rickettsiales* (*Alphaprotebacteria*) are obligate intracellular bacteria. All members of the order *Rickettsiales* can be considered metabolic parasites, their genome size was found are reduced, so they are very likely metabolic dependence on the host cell (Darby, 2007). Unlike other members, intracellular bacteria in family *Rickettsiaceae*, *Rickettsia* and *Orientia* species have a unique character in lysing host phagocytic vacuole and residing primarily in the host cytosol (Winkler, 1986; Sahni, 2013). In order for the genus *Rickettsia*, which is coccoid to rod-shaped, to survive freely in the cytosol of the host cell (Rizzoli, 2014), the doubling time is typically 8 to 12 hours (Winkler, 1990). The life cycle for *Rickettsia* consists of five steps displayed in figure 2. The whole infection process causes host cell damage and death. (Sahni, 2013; Driscool, 2017).

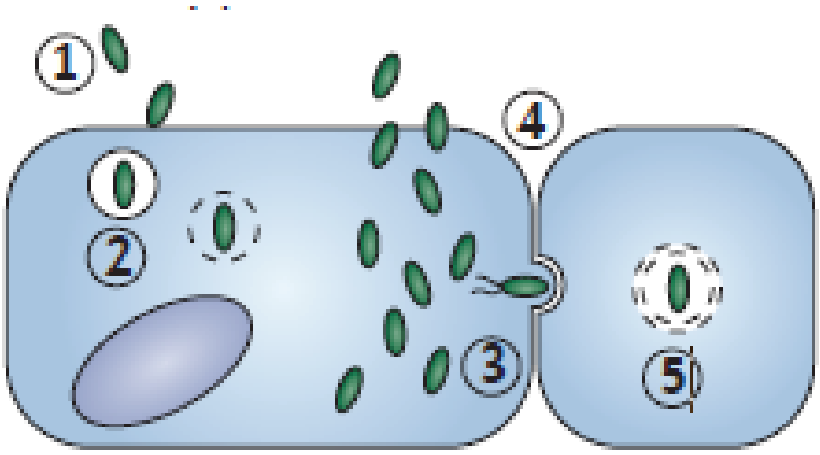

Figure 2. Lifecycle of bacteria *Rickettsia*. The life cycles of members of the Rickettsiaceae feature cytosolic replication. Members of the Rickettsiaceae induce their uptake by host cells (step 1) and once internalized, they must escape the phagosome (step 2) before replication. Next, cytosolic bacteria replicate and redistribute themselves intracellularly (step 3). To complete their life cycle, *Rickettsia* spp. lyse the host cell (step 4) or infect neighbors through intercellular spread (step 5) (Sahni, 2013).

Rickettsia in *Ixodes pacificus*

In the tick, *Rickettsia* are localized in the salivary glands and ovaries and can be transmitted to human beings through tick salivary secretions after a tick attaches to the host and takes a blood meal. If the rickettsia is pathogenic, the bitten individual may become ill.

Previous research in Dr. Zhong's lab discovered a novel species of *Rickettsia* classified as *Rickettsia* species phylotype G021 was discovered by PCR and sequencing (Phan, 2011). The median burden of phylotype G021 was 7.3 per tick cell (Cheng, 2013). Previous research in Dr. Zhong's lab also discovered the transmission routes of *Rickettsia* species phylotype G021 is through transovarial (from parent to offspring) and transstadial (from one life stage to the next life stage) passage with 100% efficiency. Even though

phylotype G021 does not have effects on embryogenesis, oviposition, and egg hatching (Kurlovs, 2014), the prevalence of phylotype G021 in *I. pacificus* ticks is 100% (Cheng, 2013). In comparisons with free-living bacteria, the data suggest that *Rickettsia* species G021 is an endosymbiont of *I. pacificus*.

In March 2013, Dr. Timothy Kurtti from the University of Minnesota isolated *Rickettsiae* from partially engorged *I. pacificus* females donated from the McKinleyville Animal Care (McKinleyville, CA). The isolate was initially named *Rickettsia* endosymbiont *Ixodes pacificus* (REIP) and cultured ex-vivo using *Ixodes ricinus* IRE11 and *Ixodes scapularis* ISE6 embryonic tick cell lines (Simser, 2002; Munderloh, 1994). The optimum temperature for the growth of REIP in ISE6 cells is 26 ºC (Kurtti, personal communications).

Introduction of Folate

Folate, also known as vitamin B9 has long been recognized as a critical cofactor in one-carbon metabolism (de Crecy-Lagard, 2007; Fenech, 2012). It represents various derivatives, which are naturally occur in foods, mostly in vegetables and fruits. Mammals cannot synthesize folate, but folate is required for one-carbon metabolism in nucleotide synthesis and methylation of DNA, RNA, protein and phospholipoids (Sybesma, 2004; Wheeler, 1992; Fenech. 2012). Because folate is essential for cell growth, a lack of folate can lead to a number of disorders. In humans, a folate deficiency can lead to cancers (de Crecy-Lagard, 2007; Pribat, 2009), heart disease (de Crecy-Lagard, 2007; Lucock, 2000) and birth defects such as spina bifida and other neural defects (de Crecy-Lagard, 2007; Wegkamp, 2007). In *E. coli,* the deletion of folate synthesis genes leads to the production of non-viable phenotypes (Fermer, 1997; Pyne, 1992). What's more, researchers found more evidence that folate plays an essential role in the growth and development of insects. For example, the folate produced by bacteria *Wigglesworthia morsitans* are essential for glossina sexual maturation and reproduction (Snyder, 2015); Although the diet of *Drosophila. melanogaster* is poor, some unknown symbiont bacteria in *Drosophila. melanogaster* produce folate allowing the fruit fly to maintain growth and development (Blatch, 2010).

Folic acid is a synthetic compound, which is structurally and functionally similar to natural folate. Although folic acid is not active as a coenzyme, but folic acid can be

converted into tetrahydrofolic acid (THF) before entering to the metabolic pathway (Figure 3).

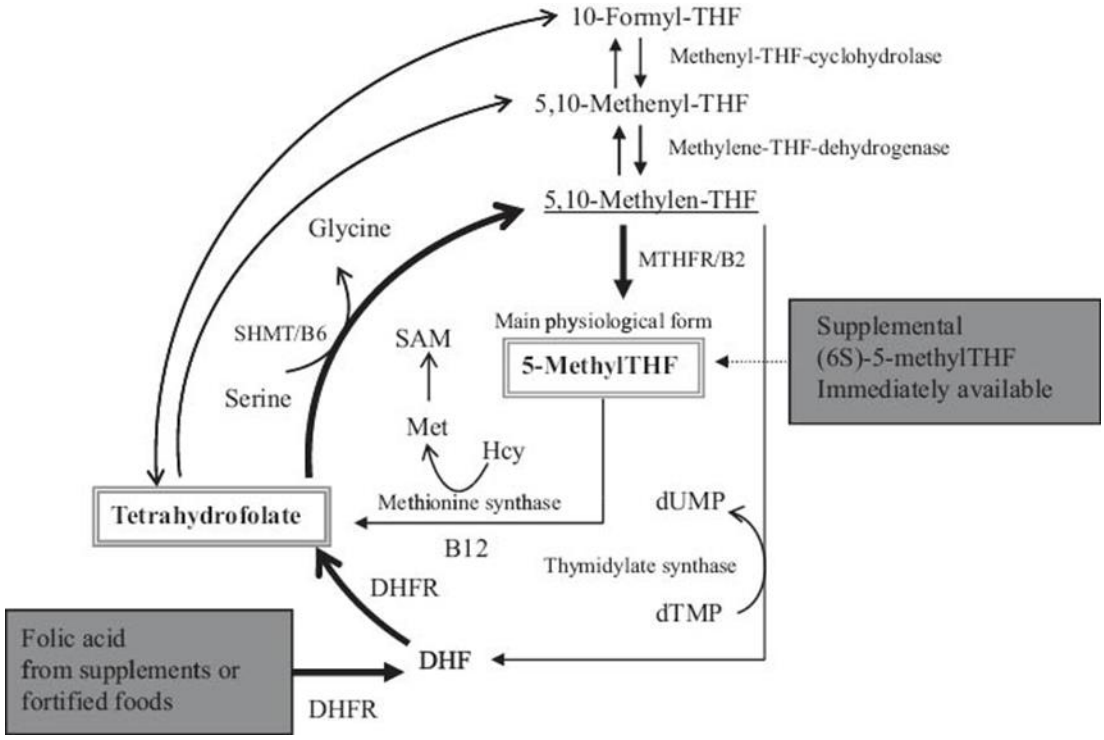

Figure 3. Folate/ folic acid metabolic pathway in plasma. "MTHFR" short for methylenetetrahydrofolate reductase, "DHFR" short for dihydrofolate reductase, "Hcy" short for homocysteine, "DHF" short for dihydrofolate, "SAM" short for S-adenosylmethionine, "Meth" short for methionine, "SHMT" short for serine hydroxymethyl transferase. The 5-MthylTHF draw our attention because it is the main physiological form in plasma (Obeid, 2013).

THF, the reduced form of the vitamin, normally synthesized in bacteria. The chemical structure displayed in Figure 4. It consists of a pterin derivative, a *p*-aminobenzoate, and glutamate moieties (Rossi, 2011; Spreadbury, 2013). THF known as an important one-carbon unit carrier in a variety of biosynthetic reactions. So THF is one active form of folate derivatives. From the inactive form of folate turn to the active form

of THF, dihydrofolate reductase is required. The one-carbon group undergoing transfer in any of three oxidation states. The most reduced form of the cofactor carries a methyl group, a more oxidized form carries a methylene group, and the most oxidized forms carry a methenyl, formyl, or formimino group. The primary source of one-carbon units for tetrahydrofolate is the carbon removed in the conversion of serine to glycine, producing N^5, N^{10}-methylenetetrahydrofolate (Spreadbury, 2013).

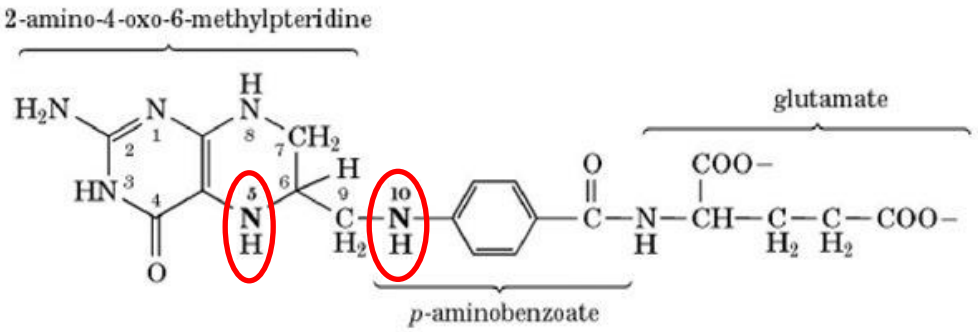

Figure 4. Chemical structure of tetrahydrofolate. THF consists of pterin derivative, p-aminobenzoate, and glutamate moieties. The N5 and N10-nitrogen atoms that can carry one-carbon functional groups circled by red color. (Spreadbury, 2013).

Different with THF, 5-methyl-5, 6, 7, 8-tetrahydrofolic acid (5-MTHF) is the major active form of folate in plasma. It acts as a methyl donor for homocysteine remethylation. The resulting tetrahydrofolate (THF) can be converted into 10-formyl-THF and then into 5, 10-Methenyl-THF then into 5,10-Methylen-THF (Figure 3). 5-MTHF occupied 95-98% of folate in serum or red blood cells. It is also known as the most available folate form in human plasma, and human whole blood (Kirsch, 2012; Obeid, 2013).

Folate Biosynthetic Pathway in *Rickettsia* Species Phylotype G021

Little is known about the nutritional basis for the symbiotic relationship of endosymbionts in ticks, though newly developed *Rickettsia ex vivo* culture systems provide the ability allow use study the novel interactions. Because adult female ticks can swell intensely during feeding (occasionally over 100 times than their unfed body body). This mean tick, especially for engorged female tick, need to synthesize a new cuticle and new cells to allow for body expansion. From a molecular-biological perspective, the tick requires more folate at this special time, since folate plays an essential role in DNA, RNA, and protein synthesis.

Previous research in Dr. Zhong's laboratory has demonstrated that *Rickettsia* species phylotype G021 contains all five genes necessary for *de novo* folate synthesis: *folE, ptpS-III, folk, folP folC,* and *folA.* Guanosine-5'-triphosphate (GTP), from tick hosts or bacterial sources, are catalyzed by a series of enzymatic actions by the, FolE, PtpS-III, FolK, FolP, FolC and FolA proteins from phylotype G021 to synthesize tetrahydrofolate (Figure 5).

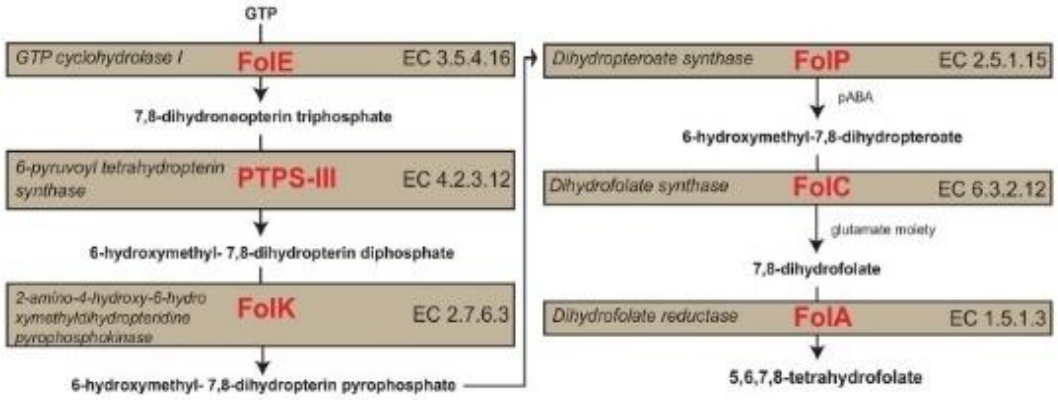

Figure 5. The proposed pathway of folate biosynthesis by *Rickettsia* species phylotype G021 in *Ixodes pacificus* (Hunter et al., 2015). First, with the exist of FolE protein (GTP-Cyclohydrolase I), GTP transfer to 7,8-dihydroneopterin triphosphate, which is a pterin-ring molecule (Hossain, 2004; El Yacoubi, 2006; Grochowski, 2007). Then PTPS-III protein, encoded by the *ptpS* gene, cleaves the side chain of 7,8-dihydroneopterin triphosphate to form 6-hydroxymethyl-7,8-dihydropterin diphosphate (Dittrich, 2008; Pribat, 2009). Then the FolKP bifunctional enzyme (2-amino-4-hydroxy-6-hydroxymethyldihydropteridine diphosphokinase and dihydropteroate synthase) will synthesis 6-hydroxymethyl-7,8-dihydropteroate by binding with the pterin ring to para-aminobenzoic acid (pABA) (Gengenbacher. 2008). A glutamate moiety is then added to 6-hydroxymethyl-7,8-dihydropteroate by FolC (dihydrofolate synthase) to synthesize 7,8-dihydrofolate, which is then utilized by the FolA protein (dihydrofolate reductase) to synthesize tetrahydrofolate (Wang, 2010).

Study the folate biosynthesis pathway might be an important first step to study the nature relationship between *I. pacificus* and phylotype G021. It may also provide a framework for identifying other potential symbiont bacteria relationship in tick. Based on the literature searching, most *Rickettsia* species from the spotted fever group and *Rickettsia belli* group have the genetic capacity to synthesize folate. However, all sequenced *Rickettisa* species from the typhus group lack the *folA*, *folK* and *folP* genes. This means those *Rickettsia* species are less likely *de novo* synthesis folate. Further digging the research, typhus group *Rickettsia* is majority found in louse and fleas. In

contrast, most of the spotted fever and *Rickettsia belli* group of *Rickettsia* are distributed in hard ticks. While it could be explained by the louse and fleas have different enzymes or other microbial symbionts in their body, which can convert 6-hydroxymethyl-7, 8-dihydropterin to tetrahydrofolate (Sahni, 2013). However, the anthropoids like hard ticks, need *de nova* symphysis folate. Back to my research project, to further confirm the hypothesis that *Rickettsia* can synthesis folate then quantify folate level is necessary.

Using Aqueous Normal Phase (ANP) to Separate Folate Derivatives

The median burden of phylotype G021 was 7.3 per tick cell (Cheng, 2013). Which means measure the folate level in tick samples is very challenge. However, we sought to use large number of *Rickettsia* infect tick cell line then quantify the folate concentration in infected tick cell line by using HPLC (High-performance liquid chromatography) or LC-MS (Liquid chromatography-mass spectrometry).

The aqueous normal phase (ANP) chromatography developed in Dr. Pesek's lab (San Jose State University) represents an important new technology for the separation of endogenous metabolites in biological matrices. ANP chromatography has a unique silica-hydride surface with a mixture of organic and aqueous solvents as mobile phases. Hydrophilic and hydrophobic compounds mixture can be both retained and separated by altering the mobile phase composition from high to low organic or vice versa. Compare with the normal phase chromatography, which is incorporates a polar stationary phase and a non-polar mobile phase in order to retain and separate polar compounds. Non-polar compounds would elute first, followed by moderately non-polar and finally polar

compounds (Hellmuth, 2011; Pesek, 2011). ANP utilizing silica-hydride-based stationary phases provide unique selectivity's for the separation of polar and non-polar compounds and offers new methods to solve difficult analytical separations (Pesek, 2007).

Silica-hydride HPLC Materials in Diamond Hydride™ Liquid Chromatography Column

The key part in ANP column is the silica-hydride materials. Silica-hydride materials are high-purity silica. It is reported with an ability to retain both polar and non-polar compounds due to its non-polar silicon-hydride (Si-H) groups on surface, instead the polar silanol groups (Si-OH) are covered the surface (Figure 6) (Pesek, 2011, Pesek, 2015).

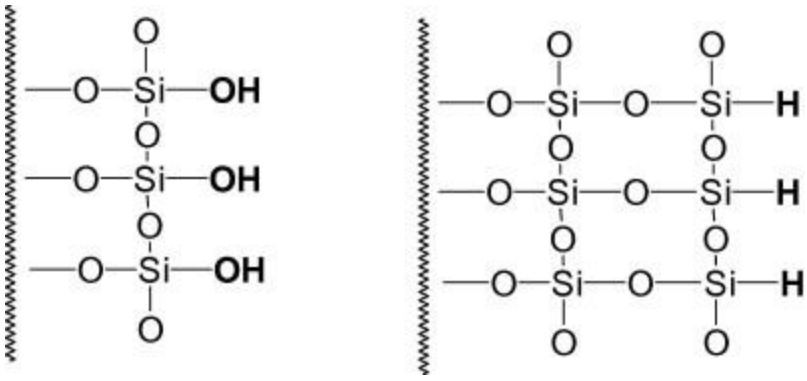

Figure 6. Compare surface structure between ordinary silica and silica hydride. The surface structure different between ordinary silica (left) and silica hydride (right) (Pesek et al., 2015).

Diamond Hydride™ materials are comprised of a small concentration of carbon (around 2%) chemically bonded to a silica hydride support. The hydride surface allows

for ANP retention while the hydrophobic attached carbon can be used in a reverse phase mechanism. In this manner, the columns can be used for retention of both hydrophilic and hydrophobic analyses depending on the mobile phase composition. The ANP conditions are especially useful in metabolomics applications (Pesek, 2009; Allahan 2009) since a given metabolome often contains a variety of polar species, which are difficult to be retained and separated by conventional reverse techniques.

Rickettsia Genetic Manipulation

A lack of basic understanding of arthropod transmitted-members of Rickettsiales in areas such as vector physiology, immune response and microbial interactions have not been addressed. The difficulty in studying *Rickettsia* spp is due to their genetic intractability. What's more, it is reported the growth rate of obligate intracellular bacteria is much slower than facultative intracellular bacteria (O'Connor, et al., 2011). Large amount work are required to purify obligate intracellular bacteria from host cells and prevent the bacteria get damage lose its biological function. What's more, the mutant obligate bacteria are needing to be selected and propagated in host cells. Then manipulate the cell invasion and survival genes are remain problematic (McClure, 2017).

In the past decades, modern molecular cell biology technologies have been developed to allow researchers to develop several methods of genetic tools to study *Rickettsia.* A few examples of such methods are replicative plasmids, transposons, homologous recombination, fluorescent protein-encoding genes, and antibiotic selectable

markers, etc. (Rachek, 1998; Agaisse., 2013; Burkhardt et al., 2011; Wood, 2012; Noriea, 2015; Driskell, 2016).

Genetic Transformation System for *Rickettsia*

Genetic manipulation methods of rickettsiae are notoriously challenging and time-consuming processes. As of Nov. 2015, only 17 peer-viewed reports have been published in the past 17 years since the first successful genetic manipulation of *Rickettsia* was published (Rachek et al., 1998; Riley et al., 2015). However, in the last two years, genetic manipulation has emerged as one of the hot topics in *Rickettsia* studies (Noriea, 2015; Schroeder et al., 2015; Riley et al., 2015; Sharma et al., 2017).

There are three major genetic manipulation methods for rickettsiae: homologous recombination, Random mutagenesis, and targeted mutagenesis (McClure, 2017).

Homologous recombination is thought as one important evolutionary mechanisms in bacterial evolution for its ability transfer a specific DNA fragment from one strain to another homologous strain (Fraser, 2007). First successful transformation experiments with *R. prowazekii* and *R. typhi* utilized homologous recombination (Rachek, 1998, 2000; Radulovic, 1999; Renesto, 2002). Using *R. prowazekii*, these authors targeted *pld* gene, encoding phospholipase D, which is thought to enable rickettsial escape from the phagosome early after uptake into a host cell. While highly significant, these early transformants were difficult to obtain, unstable during long-term culture and maintenance, and not useful for functional gene analysis since insertion was not designed to result in gene inactivation and detectable defective phenotype.

Random mutagenesis methods known as transposon insertion and chemical mutagenesis. For detail, A transposon, also known as mobile genetic material in bacteria, is a DNA sequence that can move to new positions within the genome. The key difference between a plasmid (small, circular, double-stranded DNA molecule) and a transposon is that a plasmid is a non-chromosomal DNA that replicates independently within the bacterium while transposon is a segment of chromosomal DNA that translocate within the genome of bacteria and changes the genetic sequence of the chromosome. Transposons are very likely present in all genomes, including those of Rickettsiales (Shapiro, 1999; Simser, 2005). Transposon mutagenesis does not require knowledge of the genome sequence of an organism, however, some transposons exhibit a preference for base composition of genomic DNA. From the fly *Haematobia irritans*, researchers isolate a mariner transposon (*Himar1*) which is a transposable element (Lampe, 1996) has been successfully used to mutate *Rickettsia spp*. (Reed et al., 2014; Liu et al., 2007). The *Himar1* transposase system encodes the transposase and the transposon on one or two suicide plasmids that are electroporated into host cell-free (semi-purified) bacteria. The modified *Himar1* transposase contain with antibiotic resistance cassette and fluorescent markers randomly integrates the transposon, then into AT dinucleotide sites in the bacterial genome through a cut-and-paste mechanism (Felsheim, 2006). In 2010, Clark's research group reported they used *Himar1* transposase system to restore a functional *relA/spot* gene copy to clear-plaque mutants of *R. rickettsia* Iowa and *R. rickettsia* (Both rickettsial strains can form plaques).

Targeted mutagenesis is also named site-directed mutagenesis. This mutation allows deletion or insertion a single base or multiple bases. Based on literature searching allelic exchange and mobile group II intron methods have been successfully used in *Rickettisa* species. Allelic exchange is routinely used to generate mutants in facultative intracellular bacteria and extracellular bacteria. *pld* gene was suspected as a virulence factor. And it is reported researchers have successfully inactivate the phospholipase D gene (*pld*) in obligate intracellular *R. prowazekii* (Driskell. et al.2009). They generated a *pld* mutant of virulent *R. prowazekii* strain by using linear DNA for transformation.

Then another targeted mutagenesis method is using mobile group II introns. This method requires reverse-transcribed from RNA into specific sites in the bacterial genome. So far, a commercial system named "TargeTron" is easy for researchers to operate this method. So far, it is also reported genetic manipulation is available by using mobile group II intron method has been reported successful using to genetically modify *Rickettsia Spp.* Researchers have successful knockout *OmpA* gene, a suspected virulence factor in *R. rickettsii*. And prove OmpA is not important for virulence (Noriea. et al., 2015).

In my thesis project, we use TargeTron system to knockout *folA* gene in bacteria *Rickettsia*, which method belong to targeted mutagenesis. The flow chart of the TargeTron gene knockout system is show in Figure 7. After deciding the gene we want study, a mobile group II intron piece is designed and generated from *Lactococcus lactis* L1. Due to the site-specific retroelement mechanism, this group II intron piece can invade its cognate intron-minus gene (Frazier, 2003). Through the retrohoming mechanism, the

intron lariat RNA can be inserted into a DNA target site. Then it is reverse transcribed by the associated intron encoded enzyme protein (IEP) (Lambowitz, 2004). The DNA target site is recognized primarily by base pairing of easily modified intron RNA sequences, following the intron piece can be inserted into the specific our interesting target gene (Chen, 2005), thus make the target gene unfunctional. To date, the TargeTron system has been validated in *E. coli* (Perutka, 2004), *S. aureus* (Yao, 2006), *C. perfringens* (Chen, 2005), *S. typhimurium* (Karberg, 2011) and *R. rickettsia* (Noriea, 2015).

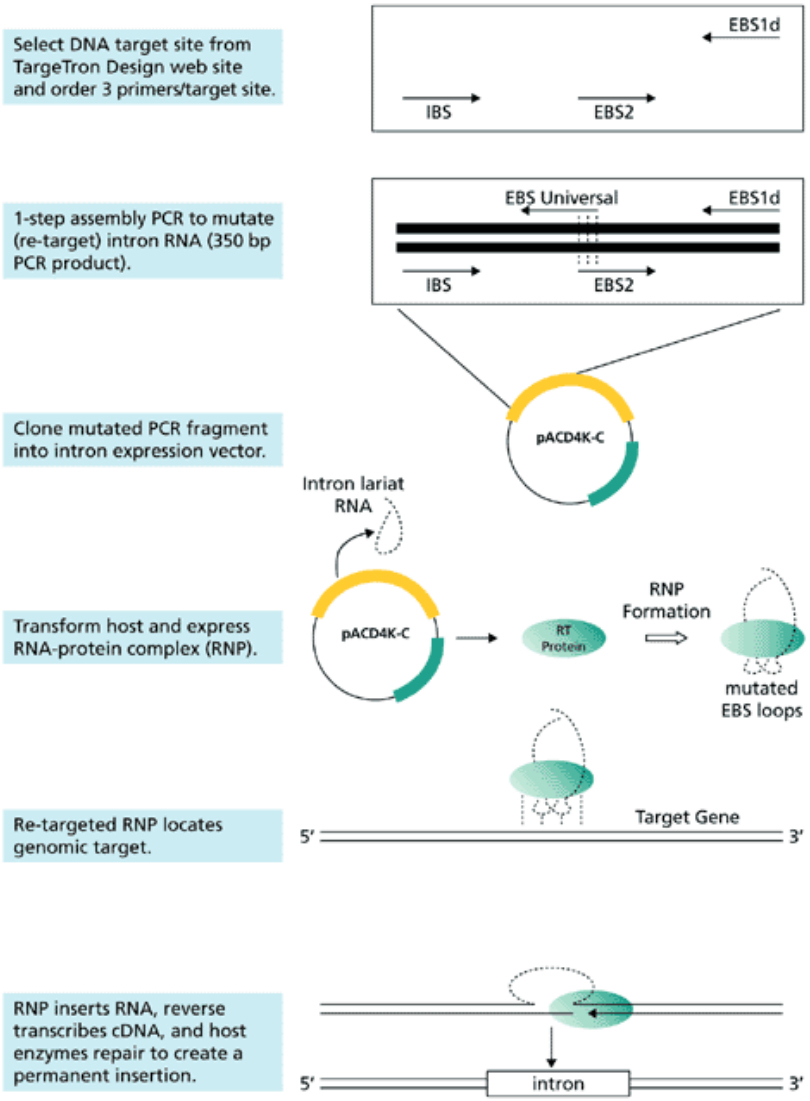

Figure 7. The TargeTron system used to knockout bacterial genes. First, the target sites in genome is calculated by computer algorithm. In normal, a 1 kb size gene can be expected to contain 5 to 11 group II intron insertion sites. Second, the computer algorithm outputs all possible primer sequences with different percentage rate. The higher percentage rate means a higher efficiency for binding. Use the selected primer set following with a PCR process will generate a 350 bp PCR fragment. This PCR fragment is ligated into the host followed by expression of the re-targeted upon chromosomal insertion. Using gene specific primers, kanamycin resistant colonies are PCR screened to confirm insertion (TargeTron® Gene knockout system user guide, Sigma-Aldrich).

Specific Aim

The nature of the relationship between REIP and *I. pacificus* is unknown. Former graduate students in Dr. Zhong's lab amplified all folate genes by PCR and demonstrated the folate genes are transcribed in both engorged and flat ticks as well as in REIP-infected ISE6 cells by RT-qPCR (Hunter, 2015; Alowaysi, 2015). Recombinant folate proteins of REIP can also be overexpressed in *E. coli* (Bodnar, 2015). The functions of the recombinant FolA and FolE proteins have been determined by *in vitro* enzymatic assays. However, we have not obtained evidence that the REIP synthesizes folate by quantitation. Therefore, in my project, I have two main goals. First, to demonstrate that folate is synthesized by REIP. Second, to construct *folA* knockout mutants using TargeTron knockout system.

To achieve the goals, three specific aims are listed:

1. Measure folate concentration in REIP infected ISE6 tick cell line.
2. Knockout *folA* gene in REIP by TargeTron knockout system.
3. Classify REIP into species and subspecies by phylogenetic tree constructions.

Most gene manipulation studies in rickettsia research have consisted of non-essential genes, such as *parA*, *dnaA* (encoding proteins important for plasmid replication, maintenance and partitioning), *rickA* (involved in rickettsial motility), *ompA,* and *ompB* (encoding the abundant spotted fever group rickettsiae outer membrane proteins). In my project, I aim to manipulate the essential gene *folA*. It has been found in *E. coli* and other

bacteria that *folA* is an essential gene for bacterial growth and survival (Zywnovanginkel, et al., 1997). Since *folA* is the last gene in the folate synthesis pathway in REIP (Hunter, et al., 2015), deletion of the *folA* gene should directly inhibit the biosynthesis of tetrahydrofolate. Since we hypothesis that REIP can synthesis folate. We hypothesize that folate starvation can trigger REIP to synthesize more folate. If the *folA* gene can be knocked out, the folate concentration produced by the mutant REIP should be decreased. The results of this study may help in understanding the symbiotic relationship between REIP and *I. pacificus* ticks. Last but not least, it is important to classify the species and subspecies of the *Rickettsia* we used in Dr. Zhong's lab.

Investigations into the endosymbiotic behavior of non-pathogenic species may also prove more productive and more effective treatment methods to decrease the incidence of tick-borne diseases such as more specific anti-folate drugs or even the creation of transgenic ticks.

MATERIALS AND METHODS

Maintain and Infect ISE6 Cell Line

Tick Cell Line ISE6

Ixodes scapularis ISE6 embryonic cell line was provided by Dr. Timothy Kurtti from the University of Minnesota. The ISE6 cells were grown in complete L-15B300 medium, supplemented with 5% fetal bovine serum, 5% tryptose phosphate broth, and 0.1% bovine lipoprotein cholesterol concentrate (Munderloh and Kurtti, 1989). Cells were cultured in 25 cm^2 monolayer flasks (Fisher Scientific, Pittsburgh, PA), incubated at 34°C, and fed on a weekly basis. Cell growth and development was monitored daily using an inverted microscope (Leica, Buffalo Grove, IL). The percent confluency of ISE6 cells was determined by comparison between the amount of space taken up by the cells, and the amount of space that was left unoccupied. ISE6 cells were counted using a hemocytometer (Reichert, Buffalo, NY) and a light microscope (Scientific Instrument Co, Sunnyvale, CA). Once the ISE6 cells reached 80% confluency, ISE6 cells were subcultured with a 1:3 ratios with fresh L-15B300 complete medium. Subcultures normally take 3 weeks to reach 80% confluency.

To generate cells from liquid nitrogen, an ampoule of frozen cells is rapidly thawed in a 37°C water bath, the cell suspension in freezing medium is added to 5 ml complete medium, and the flask is incubated over night at 34°C. The culture should be fed the next day with a complete change of growth medium. During the first week after

thawing cells, it may be desirable to include an antibiotic solution such as a mixture of penicillin (50-100 IU/ml) and streptomycin (50-100 µg/ml). Continuous use of antibiotics is not recommended, which may interfere with cell growth.

Infection of ISE6 Cells with REIP

The bacterial isolate REIP was also provided by Dr. Timothy Kurtti from the University of Minnesota. Normally a ratio of 1:20 (250 µL of the REIP lysate added into a total volume of 5 mL 80% confluency uninfected ISE6 cells) was used to infect ISE6 cells. Giemsa stain (KaryoMAX®, Thermo Fisher Scientific) was performed weekly to monitor the infection status of the ISE6 cells. Normally it takes 3-5 weeks for 80% of confluency ISE6 cells to establish a heavy infection. At this point rickettsiae could either be harvested or used to infect fresh uninfected ISE6 cells.

Giemsa Stain

Giemsa stain was used to confirm and track the infection of REIP in ISE6 cells. This stain is a mixture of methylene blue and eosin. The function of eosin is to bind to DNA phosphate groups, especially the areas with high levels of adenine-thymine (A-T) (Ellison, 2007). Giemsa stain can be used to distinguish rickettsiae from the host cell, because of the A-T rich regions of DNA. The rickettsiae are stained dark blue in contrast to the light blue stain of the surrounding host cells. To perform the Giemsa stain, the Giemsa stain (Gibco, NY, USA) was diluted with 1:20 ratio with Gurr buffer pH 6.8 (Gibco, NY, USA). Specimen were stained at room temperature for 7 mins.

Classification of REIP

To confirm that there is only one genus or genotype in the REIP isolate, *16S rRNA*, *gltA*, *ompA* genes are used for multilocus sequence typing (MLST) to detect the single nucleotide polymorphisms to distinguish *Rickettsia* species (Fournier et al., 2003; Zhu et al., 2005). However, because coding DNA may not provide enough nucleotide sequence variation to differentiate within some rickettsial species, we also used multi-spacer sequence typing (MST). This method utilizes intergenic spacers such as *dksA-xerC*, *mppA-purC*, and *rpmE-tRNA*^{fMet} and can differentiate at the intraspecies level (Fournier et al., 2007; Zhu et al., 2005). Nucleotide sequences of complete open reading frames of *16S rRNA* (accession number NZ_LAOP01000001), *gltA* (accession number KJW02430), *ompA* (accession number KJW02278), *ompB* (accession number KJW03404), *and sca4* (accession number KJW03052) of REIP obtained from NCBI are used to confirm our *16S rRNA*, *gltA*, *ompA* sequences as well as more compressive classification of the REIP isolate.

DNA Extraction, PCE and Clone

The genomic DNA was extracted from 5×10^5 REIP-infected *Ixodes ricinus* IRE11 cells using DNeasy Blood & Tissue Kit for both MLST and MST (Qiagen). *16S rRNA*, *gltA*, *ompA dksA-xerC*, *mppA-purC*, and *rpmE-tRNA*^{fMet} were amplified via PCR using primers specified in Appendix A (Simser et al., 2002; Fournier, 2007; Cheng et al., 2013b). 2μL genomic DNA (<50 ng/L), 1 μL 5 M forward and reverse primers, 10 μL

GoTaq® Green Master Mix (Promega), and 6 µL PCR grade water were added in PCR reactions. Negative controls contained all components with the exception of REIP genomic DNA. The *β-actin* gene was amplified simultaneously to serve as a positive control using *β-actin* primers and field collected *I. pacificus* (Cheng et al., 2013b). PCR reactions were performed in an Applied Biosystems 2720 Thermal Cycler (Applied Biosystems) with an initial denaturation at 95ºC for 5 minutes; this was followed by 30-45 cycles of denaturation at 95ºC for 30 seconds, annealing at 50-60ºC for 30 seconds, and extension at 72ºC for 30 seconds. The final extension was completed at 72ºC for ten minutes. Following amplification, PCR products were run on 2% agarose gel with 1X TAE buffer and stained in 10 mg/mL ethidium bromide. AlphaImager® HP was used to visualize and photograph gels (ProteinSimple). The PCR amplicon were then used in the cloning procedure. PCR amplicons were ligated into StrataClone's pSC-A-amp/kan cloning vector (Agilent Technologies). Transformants were plated on LB agar containing 100 µg/mL ampicillin and 40 µl of 2% X-gal. White colonies were then restreaked on LB/AMP/X-gal plates. Following restreaking, white colonies were grown in LB broth containing 100 mg/mL ampicillin overnight at 37ºC. Plasmids were purified by E.Z.N.A.® Plasmid Mini Kit (Omega) and constructs were confirmed by running *EcoRI* restriction enzyme digests (Promega) on 1% agarose gel with 1X TAE buffer and stained in ethidium bromide. Sequencing of the PCR amplicons was conducted by Elim Biopharmaceuticals, Inc (Hayward, CA, USA) using M13 reverse primer (5'-GGAAACAGCTATGACCATG-3'). Sequences from 30 clones of *16S rRNA*, *gltA*, *ompA*, *dksA-xerC*, *mppA-purC*, and *rpmE-tRNA*^{fMet} genes were aligned in ClustalX

version 2.1. Sequencing data determined the insert size of clones for *gltA, ompA, 16S rRNA* genes to be 382 bp, 530 bp, and 436 bp, respectively. Sequence alignments of thirty clones for each of the three genes determined that the nucleotide sequences were identical to one another in the amplified regions.

Phylogenetic Tree Constructions

To classify the REIP isolate to the genus and species levels, we took advantages of the completed genome sequence of *R. pacifica*, which was sequenced by Dr. Timothy Kurtti's lab at the University of Minnesota. The genome sequence is available in NCBI (accession number NZ_LAOP01000001). Homologous sequences of the whole open reading frame of each of the five genes of REIP, *16S rRNA* (accession number NZ_LAOP01000001), *gltA* (accession number KJW02430), *ompA* (accession number KJW02278), *ompB* (accession number KJW03404), and *sca4* (accession number KJW03052), were obtained by BLAST analysis. For phylogenetic reconstruction, homologous sequences were aligned in ClustalX version 2.1. The concatenated nucleotide sequences were translated to amino acid sequences, with the purpose of aligning the nucleotide sequences to match the amino acid alignment in Mesquite. Phylogeny of the concatenated sequence was constructed by SeaView (version 4.4.3) (http://pbil.univlyon1.fr/software/seaview.html). Since the *ompA* gene is truncated or lacking in some *Rickettsia* species, phylogeny of the *ompA* nucleotide sequence of REIP and its homologous sequences was individually constructed by SeaView. Gouy and Guindon S. & Gascuels' method was used to determine evolutionary distance values,

which were then used to construct phylograms by neighbor-joining method and maximal parsimony method (Gouy, 2009).

Measurement Folate Concentration

The Starvation Test of ISE6 Cells

Once three ISE6 flasks have reached the desired confluence level of 80%, ISE6 cells were then gently scraped and aliquoted into a 24-well plate. Each well was given 0.5 mL cell suspension. Cell plates were then incubated at 34°C for two days to allow for cell attachment to the cell plates. After two days of incubation, the old medium was removed, and the pellet was rinsed with starvation medium (0% FBS L-15B300 medium) twice. The wells were then incubated using the starvation medium.

Cell number and cell viability were determined after 0 h, 0.5-hour, 1-hour, 2-hour, 4-hour, 6-hour, 8-hour, 10-hour, and 12-hour incubation times. All analyses were run in triplicate, and the respective data obtained in each case were averaged.

Sample Preparation

Rickettsia Growth

The ISE6 cells were maintained at 34°C until an 80% cell confluency was reached. Once 80% confluence was reached REIP strains were used to infect ISE6 cell lines in L-15B300 culture medium at 26°C for two weeks. An uninfected ISE6 flask was

also cultured at 26°C as a control. Giemsa stain was used to confirm infection of the ISE6 cell line.

Prepare Cell Supernatant and Cell Pellet Sample

Cell number and cell viability in each flask were counted individually by using a hemocytometer and trypan blue staining method. Cells were gently scraped and aliquoted into centrifuge tubes. The total cell pellet was harvested by centrifugation at 13,400 x g for 10-min. Then the supernatant was transferred into a 15-mL conical tube, where a two-fold volume of ice-cold 100% acetonitrile and 5µL of 100mg/L methotrexate standard (Sigma-Aldrich) were added to the tube. The mixture was then incubated on ice for an hour and then centrifuged at high speed (13,400 x g) for another 10-min in order to allow the protein to precipitate from the solution. Afterwards the sample was filtered through 0.45 µM nylon HPLC membrane filter before being loaded into the HPLC machine.

The pellet was washed with 500µL of ice-cold PBS buffer twice to remove any remaining media. After the last wash the pellet was re-suspended in a 500µL ice-cold PBS buffer, then 5µL of 100mg/L of methotrexate sample was added to the suspension. This cell suspension was then passed through a 27-gauge needle to lyse the cells, and then sonicated for 3.5 minutes total time (4 passes at 30 seconds each and 30 seconds rests in between). After sonication a two-fold volume of ice-cold 100% acetonitrile and 5uL of 100mg/L of methotrexate standard were added to the solution. The solution was then placed on ice for 1 hour and then centrifuged at high speed (13,400 x g) for 10-min

in order to allow the protein to precipitate. Afterwards the sample was filtered through a 0.45µM nylon HPLC membrane filter before being loaded into the HPLC machine.

The Starvation Assay with the REIP isolate

Same cell supernatant and pellet sample preparation methods were used to measure the folate concentration by HPLC-UV. To achieve REIP starvation samples, old L-15B300 complete were decant, then cell flasks were washed with 4 mL 0% FBS L-15B300 medium. The samples were then washed twice and were incubated at 0% FBS L-15B300 media for 2 hours. An uninfected ISE6 sample was used as a control.

HPLC-UV

For UV-based analyses, a Hewlett-Packard (Palo Alto, CA, USA) 1200 HPLC system comprised of an auto sampler, degasser, gradient pump, and variable wavelength UV detector set at 280 nm were used. The system was interfaced with Agilent Chemstation (Santa Clara, CA, USA) software. The analytical column was 75 mm x 4.6 mm Diamond Hydride column (MicroSolv Technology Corp. Eatontown, NJ, USA) with a diameter of 4.2 µm in aqueous normal phase mode (ANP). Mobile phase A was Deionized H_2O (DI) + 10 mM formic acid buffer. Mobile phase B was 90:10 acetonitrile: DI H_2O + 10 mM formic acid buffer. All the solutions were filtered through a 0.45 µm nylon filter. The appropriate calibration curve solution was analyzed with a method consisting of an injection volume of 5 µl, a flow rate of 0.4 mL/min, and a gradient set as shown in table 1. All analyses were run in triplicate, and the respective data obtained in

each case were averages. 5-MTHF and methotrexate were identified by comparing their retention times in chromatograms of the calibration curve solutions with the appropriate peaks in percent recovery or sample extract chromatograms.

Table 1. The gradient set for HPLC-UV to separate folate.

Time (min)	% Mobile phase B
0	95
3	95
10	90
12	90
13	95
18	95

Gene Knockout by TargeTron Gene Knockout System

Plasmid Construction

The pARR plasmid vector, donated by Dr. Ted Hackstadt from Rocky Mountain Laboratories, is a derivative of the TargeTron (Sigma Aldrich) vector pACDK4-C. pACDK4-C encodes for *LtrA*, a multifunctional protein containing reverse transcriptase, DNA endonuclease and a DNA/RNA binding domain, allows the intronic RNA to be inserted at a specific DNA target site. The modified pARR vector contains a rickettsial

rpsL promotor right before multiple cloning sites that include *Hind* III and *BsrG* I sites. pARR also contains rifampin and ampicillin resistance genes for antibiotic selections after transformation (Noriea, 2015). The TargeTron software algorithm (www.sigma-genosys.com/targetron/) (Sigma Aldrich, 2008), which predicts high-specificity group II intron insertion sites in target DNA sequences, was used to design primers for appropriate sites of intron insertion into the *folA* gene of phylotype G021. Two of the best candidates chosen from the algorithm were primer sets of IBS1/2, EBS1/delta, EBS2, and EBS Universal primers (table 2). The intron DNA fragments produced by PCR were cloned into TA clone vector (Agilent Technologies, CA, USA). Then both the TA clone and the pARR plasmid were double digested with *Hind* III and *BsrG* I enzymes (New England BioLabs Inc. MA, USA). Sticky ends were generated and T4 DNA ligase (New England BioLabs Inc, MA, USA) were used to ligate the intron DNA into the pARR plasmid. Finally, the transformants were selected on LB plates with 100 ng/ml ampicillin.

To confirm the ligation, *Hind* III and *BsrG* I enzymes were used to digest the clone DNA of the transformants. Elim Biopharmaceuticals, Inc (Hayward, CA, USA) conducted sequencing of the PCR amplicons (Table 3).

Table 2. The primers sequence for *folA* gene knockout. Two highest ranked design primers were picked named 182 and 474, based on the TargeTron computer algorithm.

Primer Name	**Sequence (5'-3')**	**T_m (°C)**
182-IBS1	AAAAAAGCTTATAATTATCCTTAATGCACATA CAAGTGCGCCCAGATAGGGTG	65.5
182-EBS1d	CAGATTGTACAAATGTGGTGATAACAGATAA GTCATACAATTTAACTTACCTTTCTTTGT	63.6
182-EBS2	TGAACGCAAGTTTCTAATTTCGGTTTGCATC CGATAGAGGAAAGTGTCT	66.5
474-IBS1	AAAAAAGCTTATAATTATCCTTAACAGACATA GCGGTGCGCCCAGATAGGGTG	66.7
474-EBS1d	CAGATTGTACAAATGTGGTGATAACAGATAA GTCATAGCGACTAACTTACCTTTCTTTGT	65.0
EBS-Universal	CGAAATTAGAAACTTGCGTTCAGTAAAC	

Table 3. Primers *Seq-F* and *Seq-R* for sequence confirm plasmid construction. Additional primers designed, which can amplify both plasmid and intron sequence to check the plasmid constructed right.

Primer Name	**Sequence**
Seq-F	CAGATAAAATATTTCTAGCTAGATTTCAGT GC
Seq-R	CCAGTTAGTGTTAAGTCTTGGTAAATTCAG

Purification of REIP from Infected ISE6 Cells

Once an infection rate was over 80%, the cell suspension of ISE6 cells was passed through a 27-gauge needle to lyse the host cells' membrane, allowing the rickettsia to be released from the ISE6 cells. The lysate was then centrifuged at low speed (275 x g) for 10-min, the supernatant was further cleaned using a 5-µm syringe-driven membrane filter (Corning®, NY) and then centrifuged at high speed (13,400 x g) for another 10min. The supernatant was discarded, and the pellet was re-suspended in 1mL of ice-cold 300mM sucrose. The pellet was washed twice with 300mM sucrose and then filtered through a 2-µm syringe-driven membrane filter. The filtered solution was then centrifuged at high speed (13,400 x g) and re-suspended in 90 µL of ice cold 300mM sucrose

Transformation

A Gene Pulse® II machine (Bio Rad, Hercules, CA) was used for electroporation. For electroporation, 3µg of intron *folA* clone DNA was mixed with 90 µL of semi-purified REIP (total REIP number over 10^8) in a pre-chilled 0.1 cm gap cuvette. The settings used for the electroporation machine were 1.8 kV, 200 Ω and 25 µF.

After electroporation, complete L-15B300 medium with folinic acid (50 ng/ml) was added into the cuvette as soon as possible. Addition of folinic acid allows the mutant REIP to survive without having to produce folate itself. The electroporated rickettsia was then mixed with 1.5 mL of uninfected ISE6 cells. The mixture was then centrifuged at 700 x g for 2-min to pellet the ISE6 cells. The sample was then incubated at room

temperature for 15-min, after which the mixture was transferred to a 25-cm^2 flask containing 3.5 mL L-15B300 complete medium with ISE6 confluence cells.

Selection of *folA* Knockout REIP Mutant

In order to select for the *folA* knockout mutant, rifampicin was added to the cell culture medium. In theory, if the electroporation is successful, the rifampicin resistant gene on the pARR plasmid helps the mutant REIP to survive in the presence of rifampicin. Rifampicin in the concentration of 100 ng/ml was used to select for the mutated REIP during the nine-hour incubation after electroporation. An additional 50ng/ml folinic acid stock was also added to the L-15B300 medium.

The flask was then incubated at 26°C for 15-20 days, after which the infection could be confirmed using Giemsa stain. If Giemsa stain results confirmed presence of infection, then the DNA extraction and PCR amplification using designed *folA*-mutant primers (table 4) were carried out with the sample.

Table 4. *folA*-mutant primers for screening mutant *Rickettsia*

Primer Name	**Sequence**	**T_m (ºC)**
FolA-mutant-F	ATGAAAAATAGAAAAATCATCGGTATAATGG	59.35
FolA-mutant-R	TTACCTCCTTTTAGTAAATTTATAAATCTGATAATTA	59.14

RESULTS

ISE6 Cell Maintenance

Ixodes scapularis ISE6 embryonic cell line was successfully maintained in Dr. Zhong's lab. ISE6 cells replicate well in the complete L-15B300 medium at 34°C, normally taking 3 weeks for a 30% confluency ISE6 cells to reach 80% confluency (Figure 8). No contamination of the ISE6 cells by microbes occurred so far.

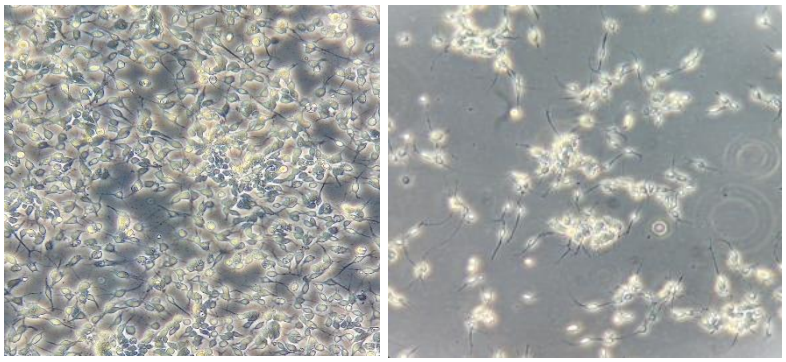

Figure 8. Observation of ISE6 cells using an inverted microscope, X40. Left) Cells at around 30% confluency. Cells have long tails with a spindle shape. Right) after three to four weeks' incubation, cells reached around 80% confluency. At this point, more cells are rounded shape

Infection of ISE6 Cells with REIP

ISE6 cell line was successfully infected with REIP. After 3 weeks post infection, morphology of REIP-infected ISE6 cells was different as that of uninfected cells. Some Infected host cells are lysed and many REIP-infected cells were observed floating. The infection status of the ISE6 cells was monitored by Giemsa stain. As shown in Figure 9,

the big dark purple structure is the nucleus of ISE6 cells and the rod-shaped bacteria observed in the cytoplasm of ISE6 cells are REIP bacteria.

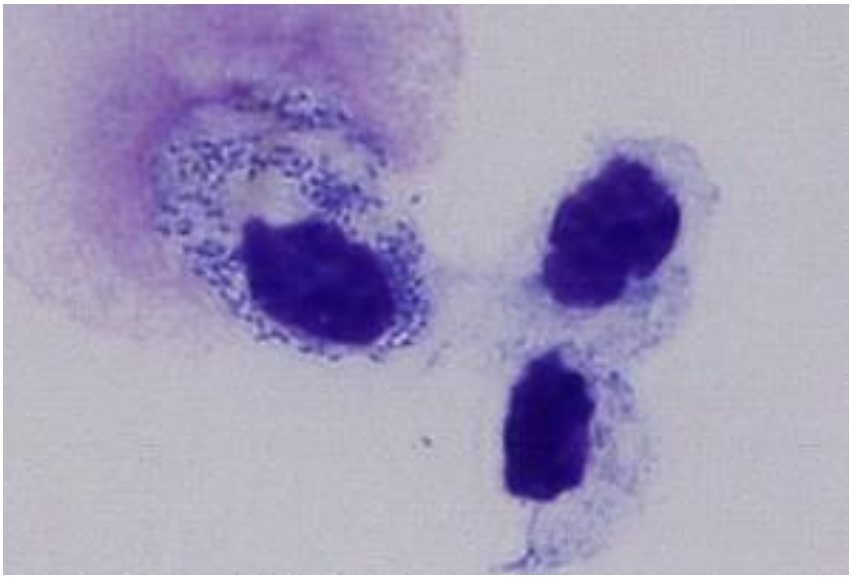

Figure 9. Giemsa stain of REIP-infected ISE6 cells after two weeks post infection. *Rickettsia* stained as dark purple rod shapes are present in the cytoplasm of ISE6 cells.

To confirm that the bacteria stained with Giemsa stain are REIP, genomic DNA of REIP was extracted from REIP-infected ISE6 cells using DNeasy Tissue Kit (Qiagen, Valencia, CA). The purified REIP DNA was used in PCR to amplify the *ompA* gene of rickettsiae (encoding an outer membrane protein of REIP). Both DNA extracted from the REIP-infected ISE6 cells and flat *I. pacificus* generated a 530 bp fragment in PCR (Figure 10), which is the expected size of the PCR amplicon of the *ompA* gene of *Rickettsia* species. DNA sequencing of the *ompA* PCR amplicon confirmed that cultured rickettsia in Dr. Zhong's lab is indeed REIP (Figure 11). It shows a 99% identify to the *ompA* of *Rickettsia* species phylotype G021 in *I. pacificus* based on the BLAST result.

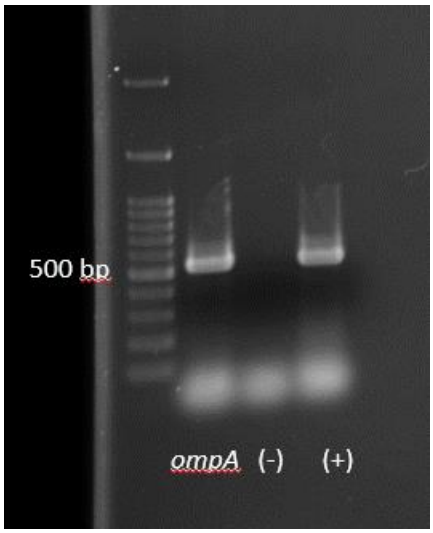

Figure 10. Gel electrophoresis of the PCR amplified *ompA* gene of REIP. Line #1: 100 bp ladder. Lane #2: PCR amplification of the *ompA* gene using DNA extracted from REIP-infected ISE6 cells. Lane #3: PCR amplification without DNA template (negative control). Lane #4: PCR amplification of the *ompA* gene using DNA extracted from flat *I. pacificus*.

Figure 11. Nucleotide BLAST result of the *ompA* PCR amplicon. Nucleotide sequence alignment of the *ompA* gene between REIP and *Rickettsia* species phylotype G021. It shows a 99% identify to the *ompA* of *Rickettsia* species phylotype G021 in *I. pacificus* (accession number GQ375161).

Rickettsia Endosymbiont *Ixodes pacificus* (REIP) is Named as *Rickettsia monacensis* subsp. *pacifica* subsp. *nov*.

Phylogenetic analysis was conducted by comparing the REIP isolate's -concatenated nucleotide sequences of *gltA*, *ompB*, *sca4*, and *16S rRNA* genes (gene sequence displayed in Appendix A) to homologous nucleotide sequences of rickettsiae available in GenBank. Trees generated from the concatenated sequence of the four genes reflected those previously generated by Dr. Zhong's lab for *Rickettsia* species phylotype G021 (Phan et al., 2011). The tree topology indicated that REIP formed a monophyletic group with *R.*

buchneri strain ISO7, *R. monacensis* strain IrR/Munich, *and R. tamurae* strain AT1. This monophyletic group forms a sister group to the rest of a clade that contains 16 spotted fever group rickettsiae. The concatenated sequences of the four genes of the spotted fever group rickettsiae are distant from the sequences of the typhus group and the *Rickettsia belli* group rickettsiae (Figure 12). Since the *ompA* gene nucleotide sequence is lacking or truncated in some *Rickettsia* species, we also constructed a phylogenetic analysis by comparing the REIP's *ompA* gene to the homologous nucleotide sequences of spotted fever group rickettsiae available in GenBank. The phylogram of the *ompA* gene confirmed that REIP was clustered in a clade with *R. buchneri* strain ISO7 and *R. monacensis* strain IrR/Munich, and forms a monophyletic group with the above two *Rickettsia* species as well as with *R. akari* strain Hartford and *R. australis* strain Cutlack (Figure 13). Both neighbor joining trees indicated that the monophyletic groups, in which REIP resides, were distinct from the rest of the spotted fever group rickettsiae. Trees generated from a maximal parsimony method also exhibited similar branching, with the exception of the *gltA* tree (data not shown). However, this discrepancy is possibly due to differences between how the two methods organize multiple sequence alignments (Saitou and Nei, 1987). We inferred that the REIP isolate shares similar evolutionary history with *R. buchneri* and *R. monacensis* due to tree topology for the concatenated and *ompA* gene sequences. As such, based on Fournier et al.'s classification scheme (Fournier et al., 2003), and our phylogenetic analyses, we propose that the REIP isolate is a novel *Rickettsia* species that is closely related to *R. buchneri* and *R. monacensis*. Therefore, we propose the name *Rickettsia monacensis* subsp. *pacifica* subsp. nov.

Previous studies have demonstrated the ability of MST to differentiate between genotypes of some *Rickettsia* species by at least one nucleotide mutation (Fournier and Raoult, 2007; Zhu et al., 2005; Znazen et al., 2013). As such, MST was used to determine possible genotypic variation present within the *R. monacensis pacifica* isolate. PCR amplification and cloning of intergenic spacers determined the insert size of *dksa-xerC*, *mppA-purC*, and *rpmE-tRNA*^{fMet} regions were 165 bp (accession number KX505844), 121 bp (accession number KX505842), and 368 bp (accession number KX505843), respectively. Analysis of thirty clones for each of the three intergenic spacers determined no variation in nucleotide sequences for the amplified regions. Considering *R. monacensis pacifica*'s nucleotide homology among all thirty clones, we assumed the isolate possessed one genotype and designated it IPO1 (*Ixodes pacificus* ovary tick 1). The neighbor-joining tree shown in Figure 14 was based on the concatenated nucleotide sequence of *dksa-xerC*, *mppA-purC*, and *rpmE-tRNA*^{fMet} regions and their homologous sequences in GenBank. The strains on the phylogenetic trees based on the sequence of *gltA-ompB-sca4*-16S and the three intergenic spacers are slightly different. This is because some of *Rickettsia* species do not have the three intergenic spacer sequences and some of *Rickettsia* species have two of the three spacer sequences in GenBank. These *Rickettsia* species are not included on the phylogram based on the nucleotide sequences of the three intergenic spacers. The phylogram of the three intergenic spacers supported the phylogeny of the concatenated sequence of the of *gltA*, *ompB*, *sca4*, and *16S rRNA* genes as well as the phylogeny of the *ompA* gene sequence; *R. monacensis pacifica* strain

IPO1, *R. monacensis* strain IrR/Munich, and *R. buchneri* strain ISO7 forms a monophyletic group that is distinct from the rest of the spotted fever group rickettsiae.

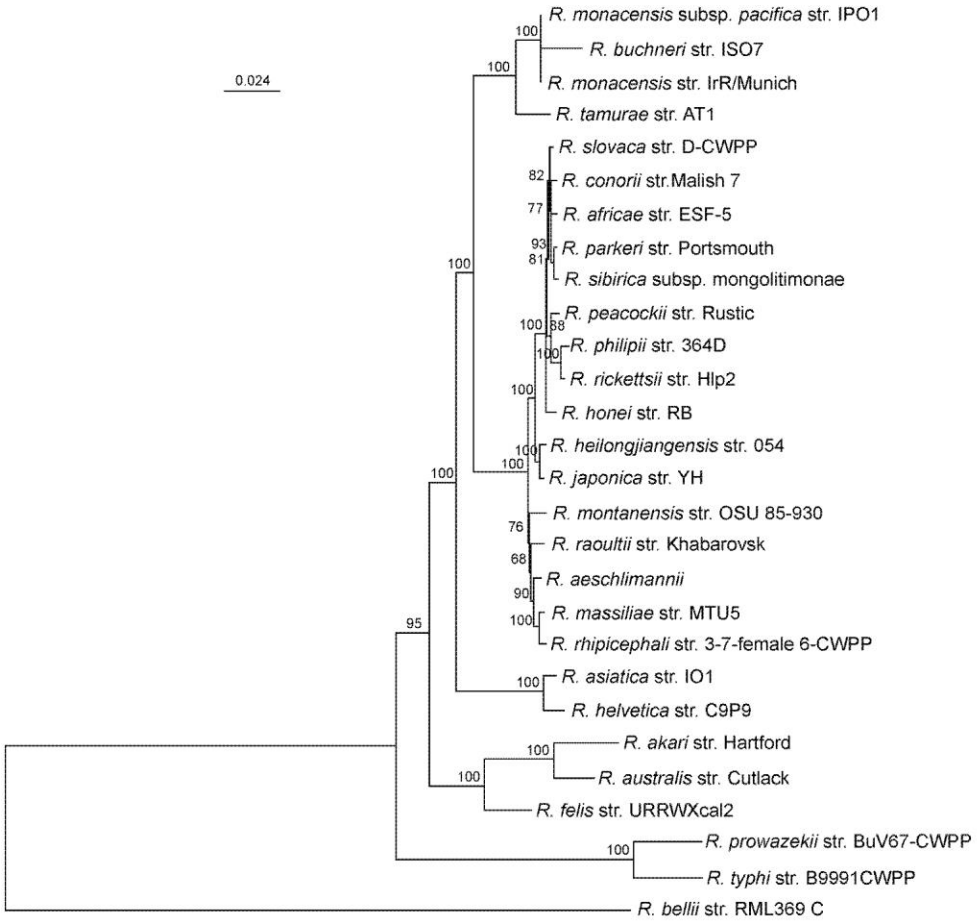

Figure 12. Phylogenetic tree of concatenated *gltA, ompB, sca4* and *16S rRNA* gene sequences of *Rickettsia monacensis pacifica*. Tree was generated using neighbor-joining distance method and 1000 bootstrap replicates. Bootstra values >50 are shown at the nodes. Bar, nucleotide distance. *R. monacensis pacifica* presented the top of the tree. Other selected sequences on the tree include: *R. aeshlimannii, R. africae, R. akari, R. asiatica, R. australis, R. bellii, R. buchneri, R. conorii, R. felis, R. heilongjiangensis, R. helvetica, R. honei, R. japonica, R. massiliae, R. monacensis, R. montanensis, R. parkeri, R. peacockii, R. philipii, R. prowazekii, R. raoultii, R. rhipicephali, R. rickettsii, R. sibirica, R. slovaca, R. tamurae,* and *R. typhi*. The accession numbers of genes of all Rickettsia species are listed in the Appendix B.

Figure 13. Phylogenetic tree of *ompA* gene of *Rickettsia monacensis pacifica*. Tree was generated using neighbor-joining distance method and 1000 bootstrap replicates. Bootstrap values >50 are shown at the nodes. Bar, nucleotide distance. *R. monacensis pacifica* (or *Rickettsia* endosymbiont *Ixodes pacificus)* is represented at the top of the tree. Other selected sequences on the tree include: *R. aeshlimannii*, *R. africae*, *R. akari*, *R. australis*, *R. buchneri*, *R. conorii*, *R. felis*, *R. heilongjiangensis*, *R. honei*, *R. japonica*, *R. massiliae*, *R. monacensis*, *R. montanensis*, *R. parkeri*, *R. peacockii*, *R. philipii*, *R. raoultii*, *R. rhipicephali*, *R. rickettsii*, *R. sibirica*, and *R. slovaca*. The accession numbers of genes of all Rickettsia species are listed in the Appendix B.

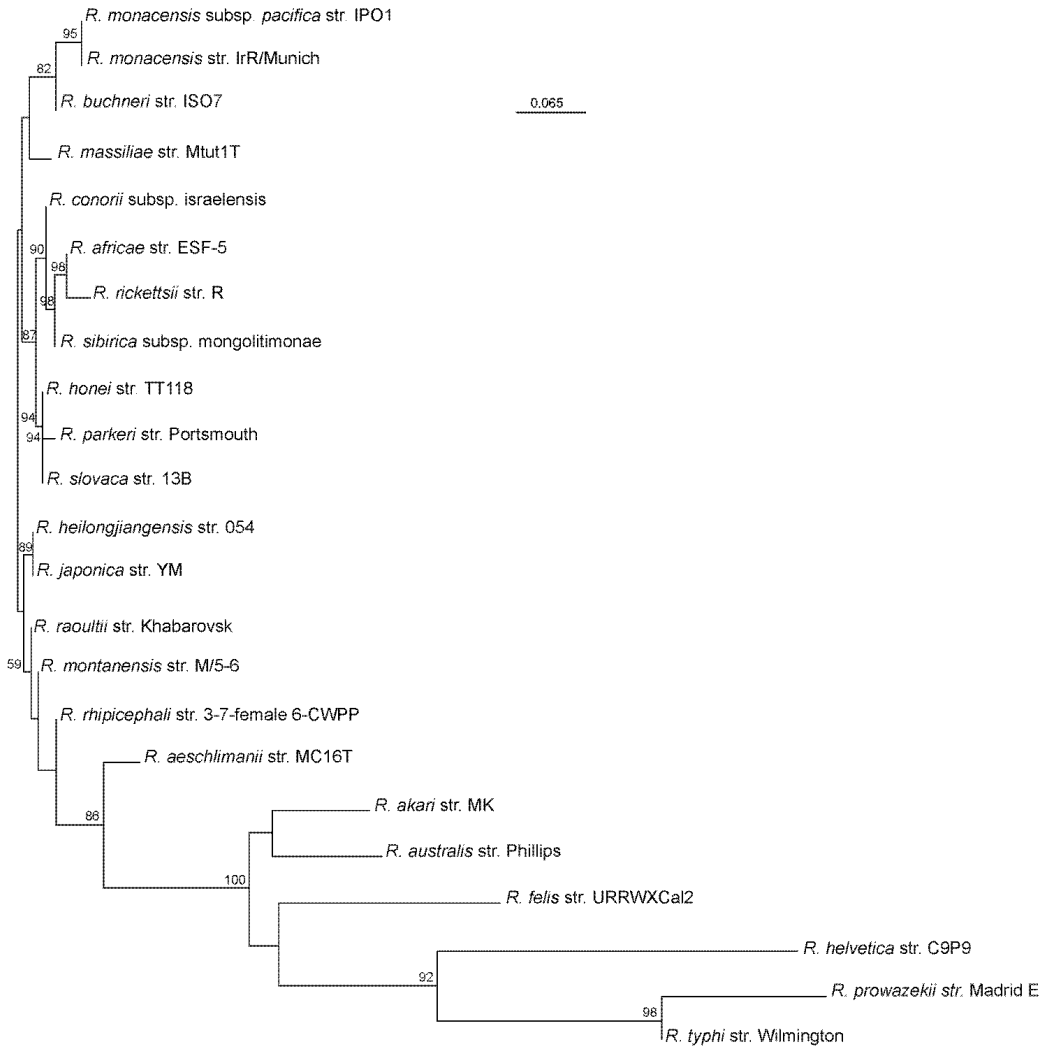

Figure 14. Phylogenetic tree of concatenated nucleotide sequence of *dksa-xerC*, *mppA-purC*, and *rpmE-tRNA^{fMet}* regions of *Rickettsia monacensis pacifica*. Tree was generated using neighbor-joining distance method and 1000 bootstrap replicates. Bootstrap values >50 are shown at the nodes. Bar, nucleotide distance. *R. monacensis pacifica* (or *Rickettsia* endosymbiont *Ixodes pacificus)* is represented at the top of the tree. Other selected sequences on the tree include: *R. aeshlimannii*, *R. africae*, *R. akari*, *R. australis*, *R. buchneri*, *R. conorii*, *R. felis*, *R. heilongjiangensis*, *R. helvetica*, *R. honei*, *R. japonica*, *R. massiliae*, *R. monacensis*, *R. montanensis*, *R. parkeri*, *R. prowazekii*, *R. raoultii*, *R. rhipicephali*, *R. rickettsii*, *R. sibirica*, *R. slovaca*, and *R. typhi*. The accession numbers of genes of all Rickettsia species are listed in the Appendix B.

The Starvation Test of ISE6 Cell line

ISE6 cells were initially incubated in the complete L-15B300 medium with 5% FBS. Cells were then cultured in the L-15B300 culture medium without FBS. Total cell number and ratio of cell death were determined at 0-hour, 0.5-hour, 1-hour, 2-hour, 4-hour, 6-hour, 8-hour, 9-hour, and 12-hour incubation after the medium change. A control group was set, ISE6 cells were incubate with complete L-15B300 medium and count cell death ratio at same time point. Our data showed the death ratio increased significantly with the incubation time from zero hour to four hours when the cells were cultured in L-15B300 culture medium without FBS. The death ratio reached 50% after 2-hr incubation. At 4-hr incubation, the cell death ratio was determined to be 60% (Figure 15, raw data are show in Appendix C).

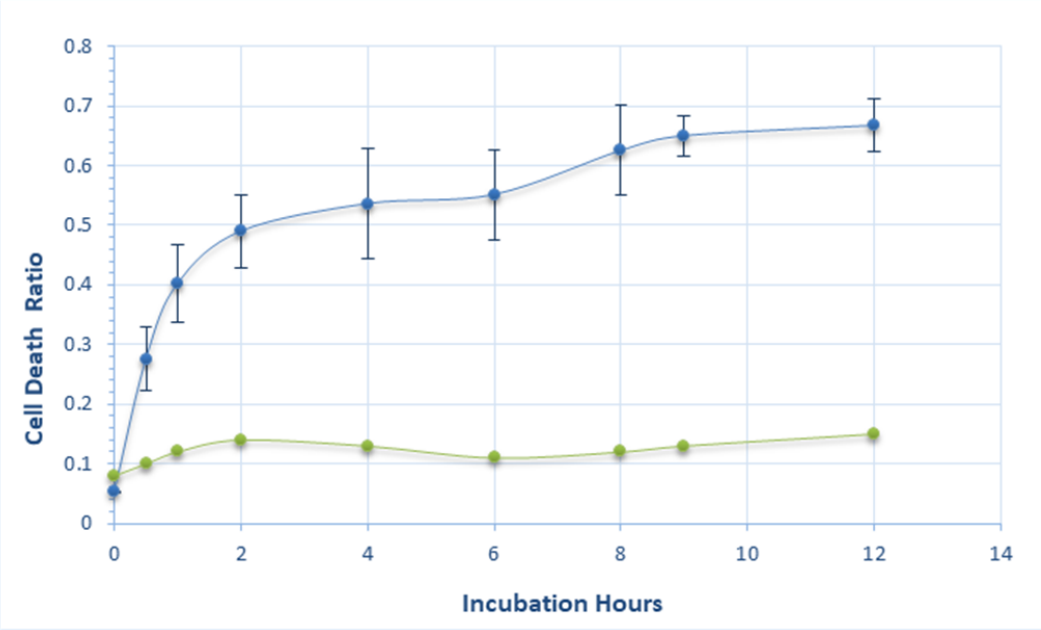

Figure 15. Compare death ratio of the ISE6 cells growing in complete L-15B300 medium and L-15B300 medium without FBS. Blue color line shows the death ratio of ISE6 cells under starvation treatment and the green line show the death ratio of ISE6 cells grow with complete L-15B300 medium. Cell death ratio were counted every two hours. Note. The 10th hour were counted at 9th hour by human error.

Measurement of the Folate Concentration by HPLC-UV

HPLC-UV Method Setup

Folic acid (Sigma- Aldrich), 5-formyltetetrahydrofolate acid (Sigma- Aldrich), 5-methyltetetrahydrofolate acid (Sigma- Aldrich) were used as standards in HPLC, whiles methotrexate was used as an internal-standard (Sigma- Aldrich). A good resolution was achieved after using an Agilent 1200 series instrument detector with a 75 x 4.6 mm Diamond Hydride column and 0.1% formic acid buffer as mobile phase. Each standard showed a clear separation from the internal-standard (Figure 16). The gradient was

performed in the aqueous normal phase mode (ANP) of separation where polar compounds (both methotrexate and folic acid have polar moieties) were retained when the mobile phase was highly organic and eluted when the gradient was changed to high aqueous (low organic) percentages. We were able to improve retention and separation of each compound within a reasonable time frame. 5-formyltetetrahydrofolate acid standard peak appeared at 9.6-9.7 min. Folic acid standard appeared at 9.6-9.7 min. 5-methyltetetrahydrofolate acid standard peak appeared at 12.2 min. Finally, the internal standard methotrexate appeared at 12.0 min.

Since 5-methyltetrahydrofolate acid is the active form of folate in plasma, we focused on measurement of 5-methyletrahydrofolate acid concentration in our specimen. A standard curve was constructed (the linear range from 0.125 mg/L to 2 mg/L). The HPLC-UV's lowest limit detection of 5-methyletrahydrofolate acid was determined to be 0.125 mg/L (Figure 17).

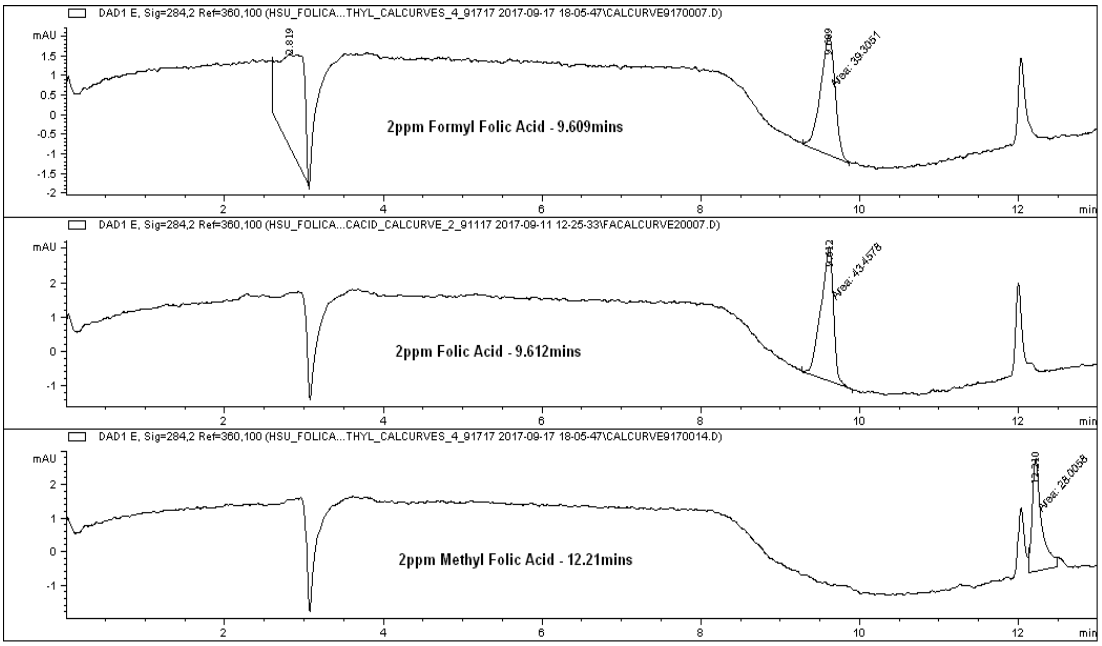

Figure 16. HPLC chromatograms of folic acid, 5-formyltetetrahydrofolate acid, 5-methyltetetrahydrofolate acid, and methotrexate internal-standard. Top) 5-formyltetetrahydrofolate (peak shown at 9.6-9.7 min) and methotrexate (12.0 min) are separated by HPLC. Middle) Folic acid (9.6-9.7 min) is separated from methotrexate by HPLC. Bottom) 5-methyltetetrahydrofolate acid (12.2 min) and the internal standard is separated by HPLC.

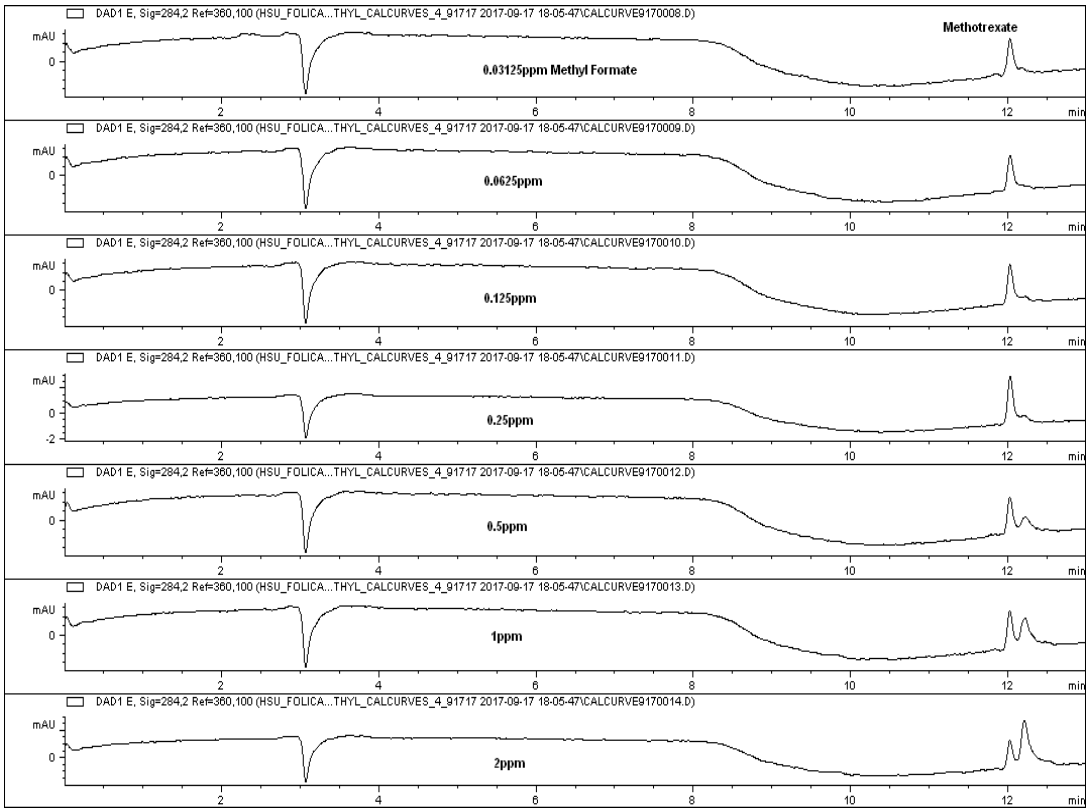

Figure 17. Quantitation of different concentrations of 5-methyltetrahydrofolate acid by HPLC-UV. The lowest concentration of 5-methyltetrahydrofolate acid that showed a peak was 0.125ppm.

Measurement of the Folate Concentration by HPLC-UV

Based on the folate standards, a standard curve was constructed. With the peak surface area converted into folate level (mg/L), the simple linear regression equation was built: $Y=0.0708X-0.0678$, $R^2=0.9854$. X means the peak area and Y for the concentration (Figure 18).

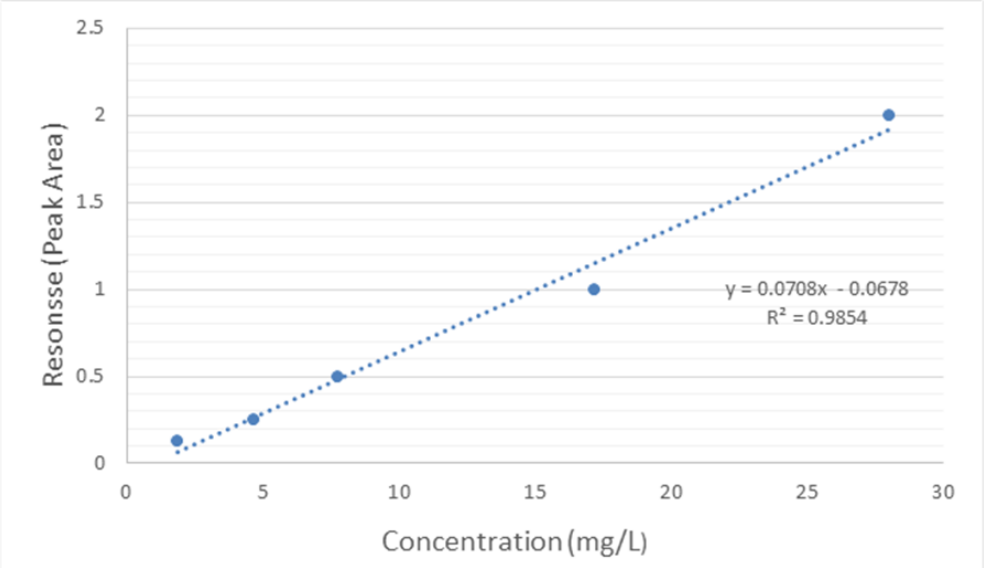

Figure 18. The standard curve for quantitation of 5-methyltetrahydrofolate acid by HPLC-UV. The simple linear regression equation for 5-methyltetrahydrofolate acid standard is shown in the figure.

Measurement of the Folate Concentration in L-15B300 medium

The folate concentrations of in 0% FBS and 5% FBS L-15B300 medium were measured. In 5% FBS L-15B300 medium, there was a peak at 12.128 min with a peak area of 5.01753, which was converted to the folate level of 0.287 mg/L. However, the peak around 12min was not present in the 0% FBS L-15B300 medium (Figure 19).

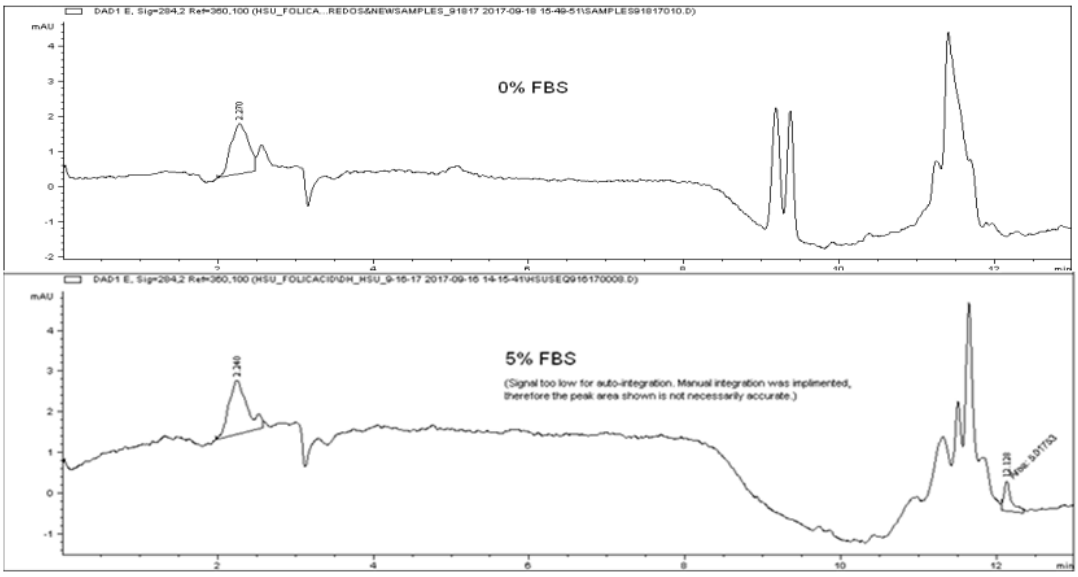

Figure 19. Comparison of HPLC chromatograms between 0% FBS L-15B300 medium and 5% FBS L-15B300 medium. A 12.128 min peak is only present in the 5% FBS medium, which is equal to the concentration of 0.287 mg/L.

Cell Counting Before HPLC Detection

Each sample flask was gently scraped and pipetted well. 45 µL cell suspension was mixed with 5 µL 0.5% Trypan blue. The total cell number and cell viability were determined afterwards, as shown in the table 5 (Summary data shown in table 5, Raw data shown in Appendix D).

Table 5. Cell number and cell viability were counted for each sample. All starvation treated samples showed decreased cell viability after a two-hour starvation treatment, especially for the uninfected ISE6 cell sample

Sample	**Total cell number**	**Cell viability**
ISE6-1	$1.18*10^6$	96.61%
ISE6-2	$1.78*10^6$	97.75%
ISE6-3	$0.96*10^6$	97.92%
REIP-1	$1.8*10^6$	97.78%
REIP-2	$1.27*10^6$	96.54%
REIP-3	$1.2*10^6$	98.33%
REIP-Starvation-1	$1.97*10^6$	94.92%
REIP-Starvation-2	$1.59*10^6$	94.24%
REIP-Starvation-3	$1.92*10^6$	94.78%
ISE6-starvation	$1.27*10^6$	89.62%

Measurement of the Folate Level in Supernatant and Pellet of REIP-infected and Uninfected ISE6 Cells

Based on the total cell numbers in each sample flask, folate level was converted to mg per liter per 10^6 cells (mg/L/10^6 cells). There was no obvious peak of 5-methyletetrahydrofolate acid (shown around 12.2 min) in both infected and uninfected supernatant samples (Figure 20).

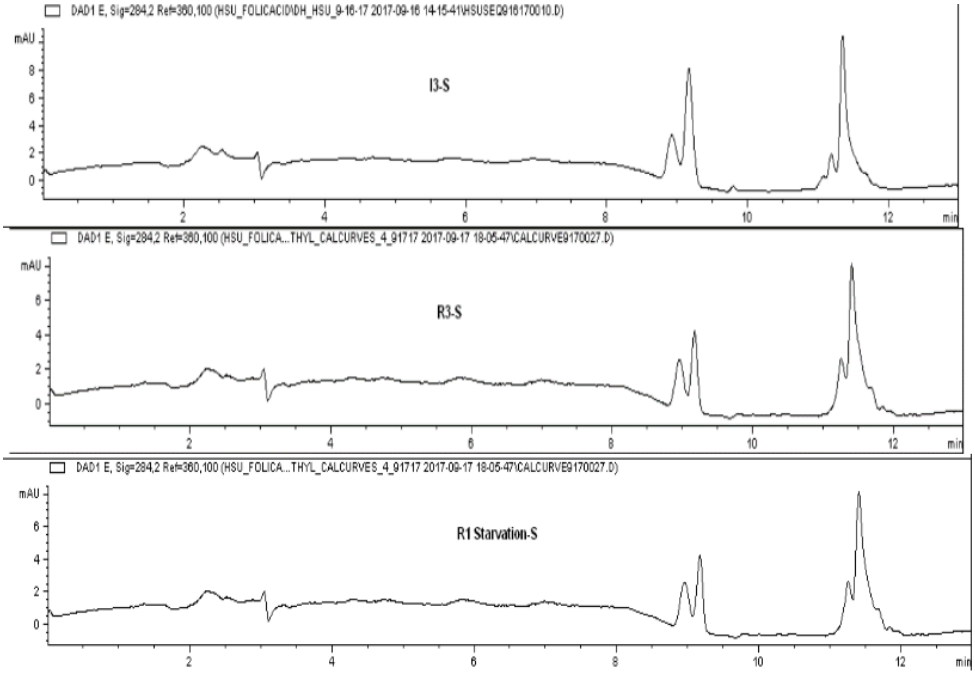

Figure 20. Comparison of HPLC chromatograms of supernatant samples from uninfected ISE6 cells, REIP-infected ISE6 cells, and REIP-infected starvation sample. I3-S stands for ISE6-3rd replication-supernatant. R3-S stands for REIP-infected-3rd replication-supernatant. R1 Starvation-S stands for REIP-infected-starvation-supernatant.

When pellets from uninfected ISE6 cells, REIP-infected ISE6 cells, and REIP-infected starvation samples were detected by HPLC for measuring the folate

concentration, the 5-methyltetrahydrofolate acid peak was present on all HPLC chromatograms. All pellet samples had a peak around 12.2 min. The tallest peak of 5-MTHF among all samples was detected in the REIP-starvation-pellet (2nd replicate), which was converted to the folate concentration of 0.6159 mg/L/10^6 cells. The folate concentration in the uninfected ISE6 pellet was determined to be 0.0707 mg/L/10^6 cells, whiles the folate concentration in the REIP infected ISE6 cell pellet was 0.1435 mg/L/10^6 cells (Figure 21). All samples were averaged and compared, as shown in figure 22 (Raw data shown in Appendix E).

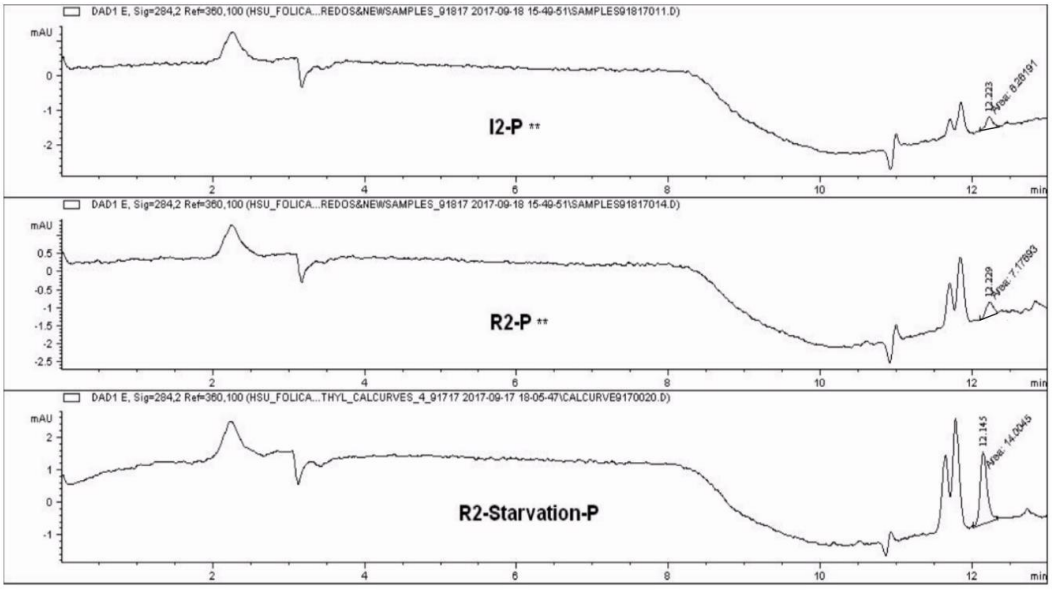

Figure 21. Comparison of HPLC chromatograms of pellet samples from uninfected ISE6 cells, REIP-infected ISE6 cells, and REIP-infected starvation sample. In ISE6 pellet sample, the 5-MTHF peak was showed at 12.223 min, which was converted to the folate level of 0.0707 mg/L/10^6 cells. In REIP-infected pellet sample, the peak was showed at 12.229 min, which was converted to the folate level of 0.1435 mg/L/10^6 cells. The REIP-infected sample with a two-hour starvation treatment showed a peak at 12.145 min, which was converted to the folate level of 0.6159 mg/L/10^6 cells.

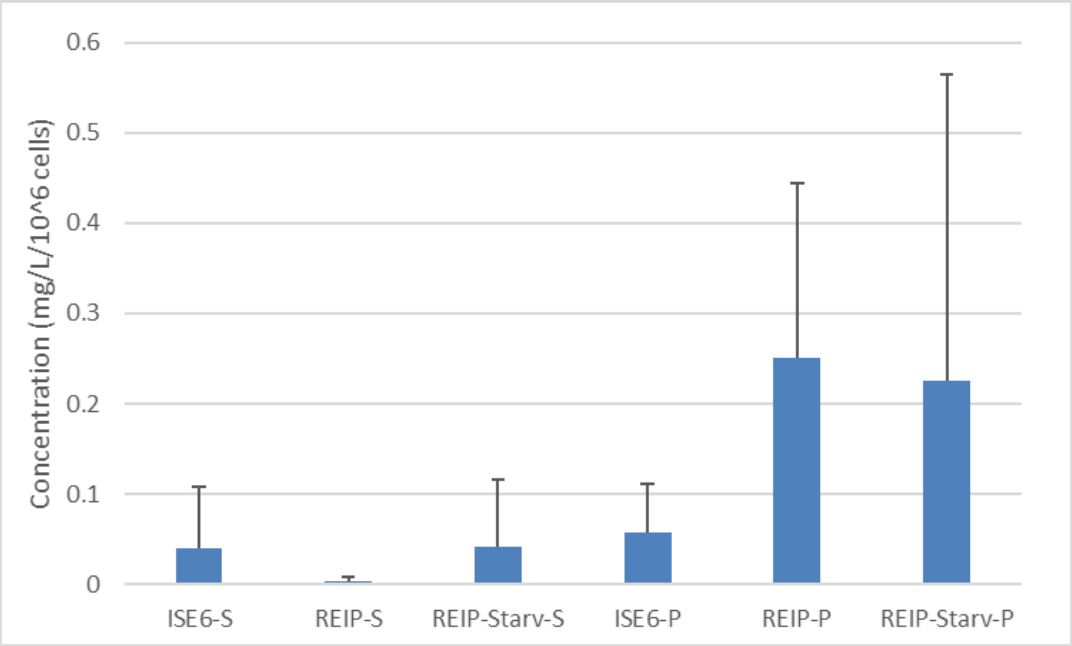

Figure 22. Comparison of averaged folate concentrations in uninfected ISE6 cells, REIP-infected ISE6 cells, and REIP-infected starvation samples. Samples included were ISE6 uninfected cell supernatant, ISE6 uninfected cell pellet, REIP infected cell supernatant, REIP infected cell pellet, REIP infected starvation treated supernatant, REIP infected starvation treated pellet and ISE6 starvation treated pellet. The p-value between ISE6-P and REIP-P is 0.05; between ISE6-P and REIP-Starv-P is 0.5; between REIP-P and REIP-Starv-P is 0.8; and between REIP-S and REIP-P is 0.05 (Raw data shown in Appendix E).

To test if the different concentrations of folate in uninfected ISE6 cells, REIP-infected ISE6 cells, and REIP-infected starvation samples had statistical significance, we performed Wilcoxon-mann-whiteney test. The p-value between the ISE6 uninfected cell pellet and REIP infected cell pellet was 0.05, meaning that the difference of the folate concentrations between two samples was statistically significant. The p-value between the ISE6 uninfected cell pellet and REIP-infected starvation was 0.5. However, the p-value between the REIP infected pellet and REIP infected starvation treated pellet was

0.8 (Figure 23). In addition, the p-value between the REIP infected supernatant samples and REIP infected pellet samples was 0.05, meaning the difference was significant. However, the p-value between the REIP infected starvation supernatant samples and pellet samples was 0.2 (Figure 24). For all supernatant samples, the 5% FBS complete L-15B300 medium showed a highest folate level. The Wilcoxon-mann-whiteney test showed that the different concentrations of folate in supernatant of all samples were not statistically significant (P>0.05) (Figure 25).

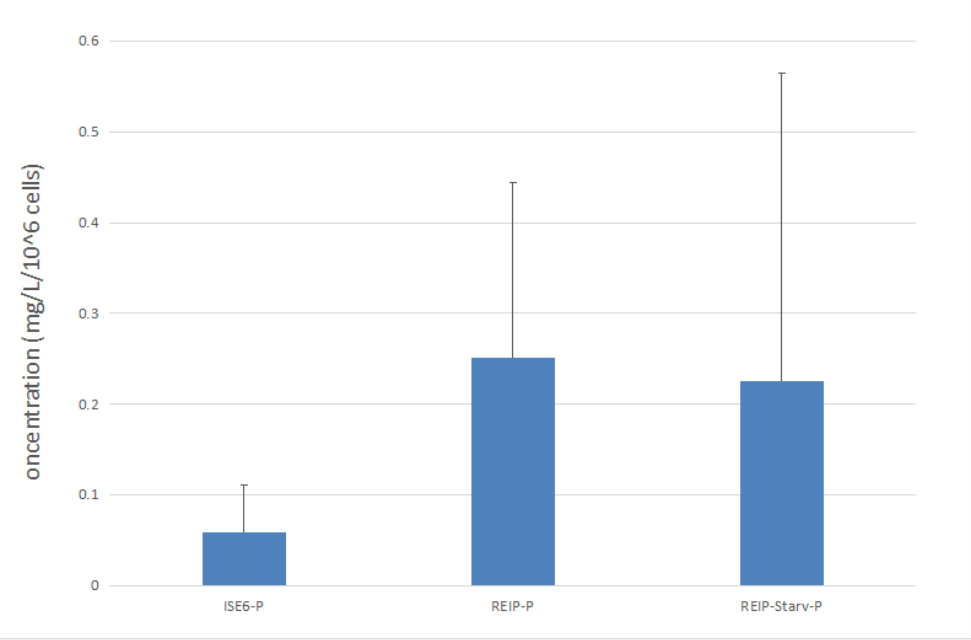

Figure 23. The folate concentrations in pellets of uninfected ISE6 cells, REIP-infected ISE6 cells, and REIP-infected starvation samples. The P-value between ISE6-P and REIP-P is 0.05; ISE6-P and REIP-Starv-P is 0.5; REIP-P and REIP-Starv-P is 0.8.

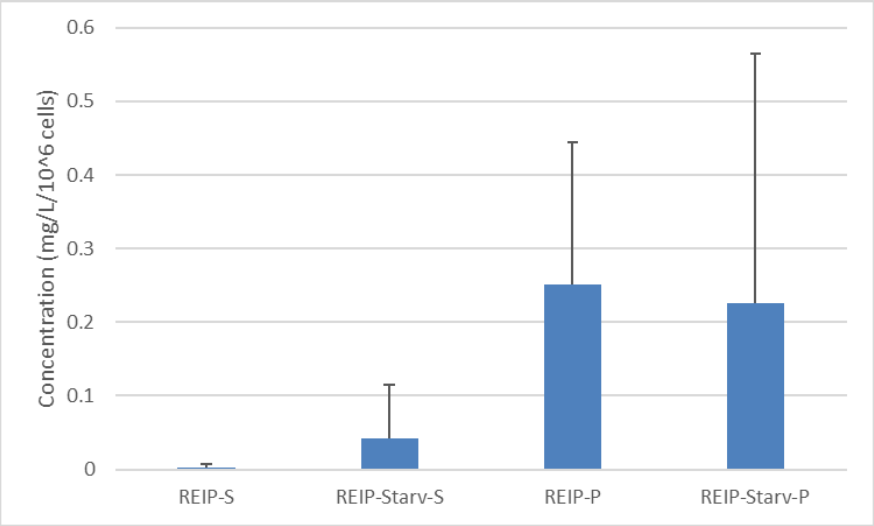

Figure 24. Comparison folate level between REIP infected supernatant and REIP infected pellet samples. P-value between REIP-S and REIP-P is 0.05; REIP-Starv-S and REIP-P is 0.2.

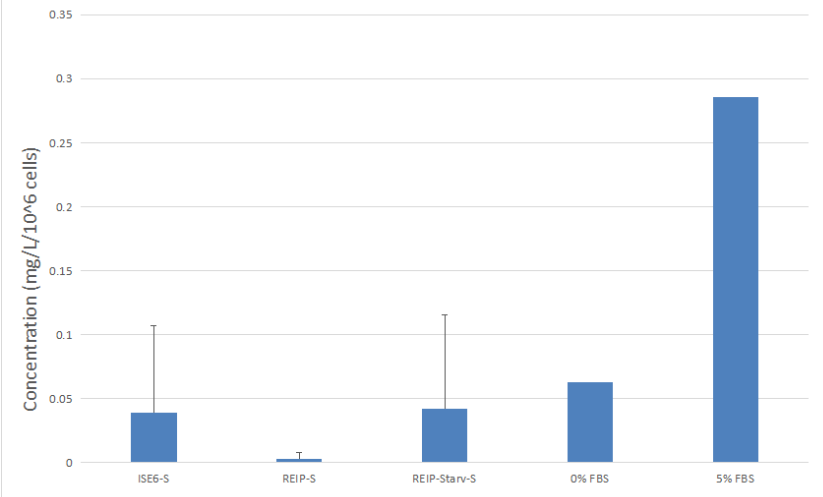

Figure 25. The folate concentrations in supernatant of uninfected ISE6 cells, REIP-infected ISE6 cells, and REIP-infected starvation samples. "0% FBS" stands for L-15B300 medium without FBS. "5% FBS" stands for L-15B300 medium contain 5% FBS. "ISE6-S" stands for ISE6 uninfected cell supernatant. "REIP-S" stands for REIP infected cell supernatant. "REIP-starvation-S" stands for REIP infected cell with starvation treatment supernatant.

Construction of *folA* Gene Knockout Mutant of REIP

Plasmid Construction

First, TargeTron computer algorithm (http://www.sigmaaldrich.com/life-science/functional-genomics-and-rnai/targetron.html) was used to identify target sites in *folA* gene for inserting the group II intron. The *folA* gene nucleotide sequence was copied and pasted into the algorithm, the highest-ranking primers that met the company's criteria were picked. Based on the *folA* gene sequence, two *folA* mutant primer sets of 182 and 474 (IBS1/2, EBS1/delta, and EBS2) were designed by the TargeTron computer algorithm. A 350 bp intron fragment was amplified after PCR with a total of four primers (IBS1/2, EBS1/delta, EBS2 and EBS Universal primers) and the intron PCR template (provided in TargeTron gene knockout kit). An *E. coli lacZ* gene control can be used to test the kit performance, works as positive control here (Figure 26).

Figure 26. Both "182" and "474" primer design amplified a 350 bp PCR fragment. TargeTron primers of either 182 or 474 amplified a 350 bp DNA fragment by PCR. The 350 bp band was the expected intron base pair size. *lacZ* control works as a positive control.

Both 182 and 474 primer sets amplified the 350 bp PCR fragments. The 350 bp intron from either 182 or 474 primer sets was successfully gel purified by Qiagen QIAquick gel extraction kit (Qiagen) and ligated with 6536 bp pARR vector. The constructions of the two intron clones were confirmed by restriction enzyme digestions using *Hind* III and *BsrG* I enzymes (Figure 27). The two intron clones were further confirmed by PCR using *Seq-F* and *Seq-R* primers. The size of the PCR fragments was 350 bp when either 474-IBS&EBS1d primer set or 182IBS&EBS1d primer set were used in PCR. The size of the PCR fragment was 714 bp when either Seq-F&R primer set or Seq-F&R primer sets were used in PCR (Figure 28). In addition, the nucleotide sequences of the intron clones were confirmed by sequencing reactions performed in Elim biopharma Inc (Hayward, CA). The nucleotide sequences obtained from Elim Biopharma Inc. after BLAST we confirmed both 474 and 182 intron clones were successfully constructed, all "N" nucleotide sequence in pARR plasma were replaced with "474" or "182" specific nucleotide sequence (Appendix F, Primer sequence shown in Table 2). Based on the BLAST search, the nucleotide sequence identity between the "182"-*folA* intron clone and TargeTron expression vector pACD4K-C is 97% and the "474"-*folA* intron clone and TargeTron expression vector pACDK4K-C is 96%. A complete plasmid map of the pARR plasmid vector is shown in Figure 29.

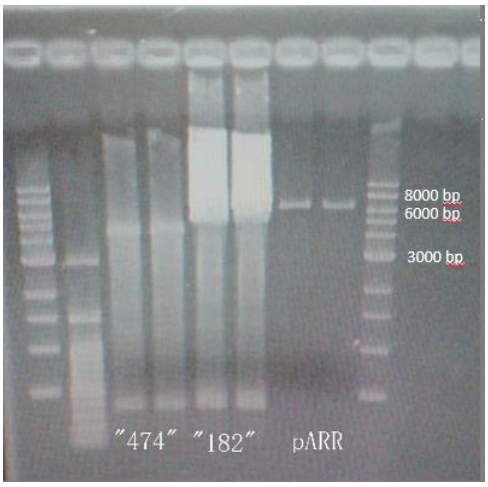

Figure 27. The restriction enzyme digestions of the clones using *Hind* III and *BsrG* I enzymes. Lane 3 & 4 are "474" intron clones. Lane 5 & 6 are "182" intron clones. Lane 7 & 8 are empty *pARR* plasmid as a control.

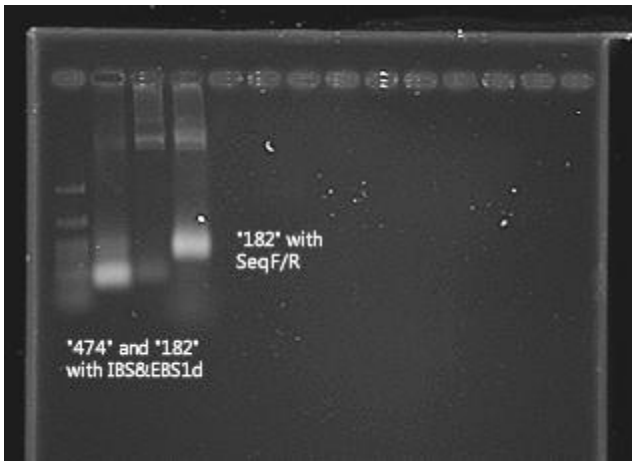

Figure 28. PCR amplifications of the intron clones. Lane 1: 100bp ladder were loaded. Lane 2: 474-*IBS&EBS1d* primer set. Lane 3: *182IBS&EBS1d* primer set. Lane 4: "182" plasmid with *Seq-F&R* primer set. *Seq-F&R* amplified a 714 bp DNA fragment.

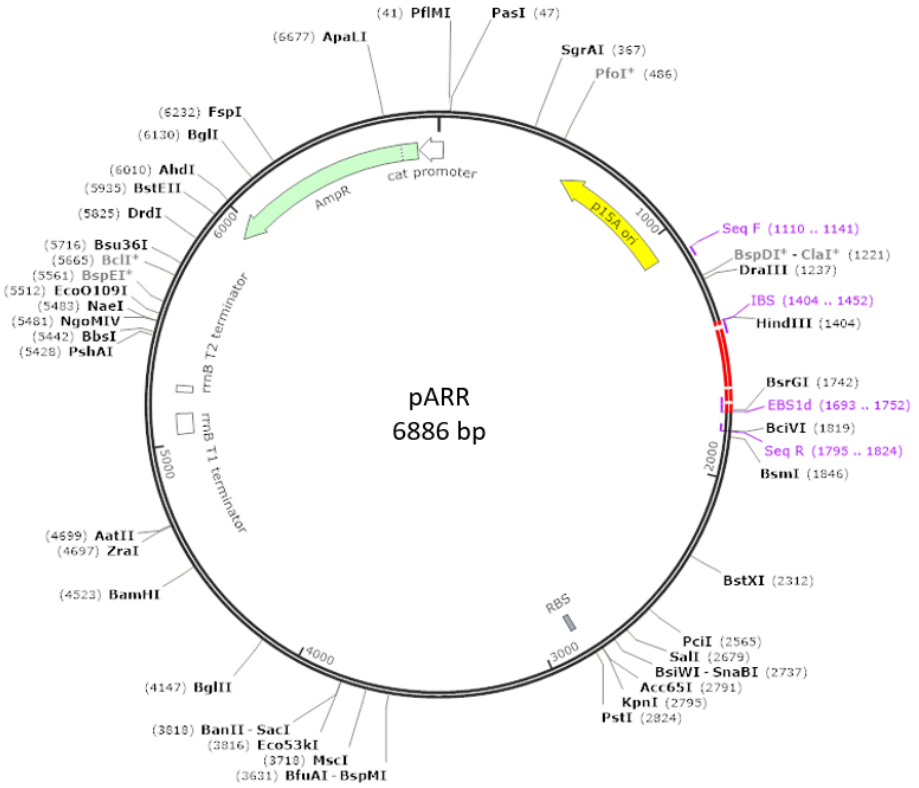

Figure 29. The plasmid vector map of pARR. The plasmid is 6886 bp. The red color part is the intron insert site. The intron piece was cloned in a TA vector first, which was double digested by *Hind* III and *BsrG* I enzyme. After gel purification, the intron DNA was ligated with double digested and pre-dephosphorylated pARR vector. The vector and intron DNA were ligated with T4 ligase enzyme. The 350bp intron sequence shown in Appendix G.

Screening of the *folA* Knockout Mutant by PCR Amplification of the *folA* Gene

After electroporation of REIP with the intro clone, REIP were cultured in complete L-15B300 medium containing rifampicin and folinic acid. The mutant REIP is selected by rifampicin. After 21 days incubation, Giemsa stain was used to confirm the presence of bacterial infection in ISE6 cells. Then DNA was extracted from REIP-infected ISE6 cells and used as the template to amplify the *folA* gene of REIP with *folA*-mutant primer by PCR (Figure 30). The size of the *folA* amplicon amplified from wild type REIP is 642 bp. If group II intron is successful inserted, the size of the *folA* amplicon is expected to be around 992 bp. However, as shown in figure 30, the sizes of two amplified PCR amplicons are 642 bp and 1.2kb. The 1.2 kb band was gel purified by Qiagen QIAquick. However, the band was not successfully gel purified due to the low amount. When the solution containing gel purified DNA was used in another PCR using *folA*-mutant primers, the 642 bp amplicon were amplified (data not shown).

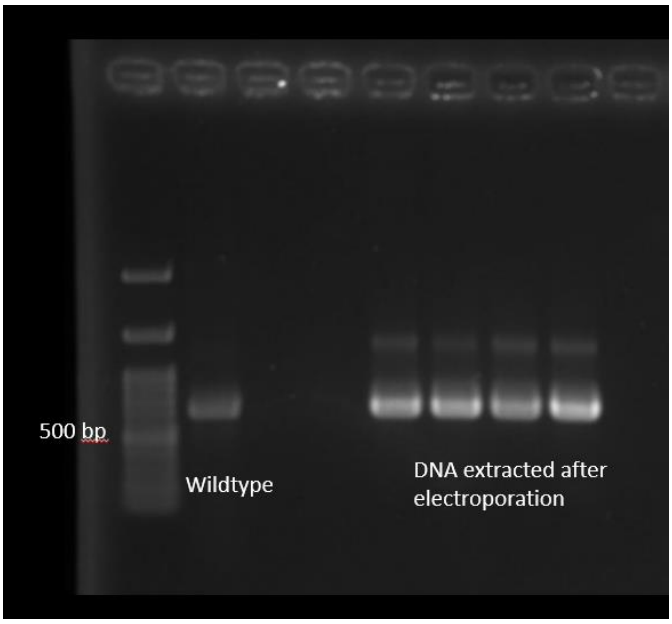

Figure 30. PCR amplification of the *folA* gene of REIP using *folA*-mutant primer. Lane 1, 100bp ladder. Lane 2, PCR amplification by using DNA extract from wild type REIP. Lane 5 to 8, PCR amplifications using DNA extract from rickettsia after electroporation.

CONCLUSION AND DISCUSSION

Tick-borne diseases remain as a serious public health issue in the United States. Evidence has shown that climate warming is changing the distribution of *Ixodes* ticks (Dahlgren et al., 2016). The incidence of anaplasmosis has increased 12-fold in the last decade (Bakken, 2015). Decreasing the prevalence of tick-borne diseases will be a daunting challenge, which requires the development of new technologies to control tick populations. The new developments of the tick control measures are only possible by furthering our understanding of the physiology of ticks. Nonpathogenic bacterial endosymbionts have been shown to contribute to their arthropod hosts' fitness by supplying them with essential vitamins and amino acids (Sakurai et al., 2005; Perlam et al., 2006; Douglas. 2007). Little is known about the nutritional basis for the symbiotic relationship of endosymbionts in ticks. Therefore, in this study, we are trying to gain a better understanding of tick biology and physiology through its endosymbiont relationship. Previous research in Dr. Zhong's lab has demonstrated that all five folate biosynthesis genes exist in the genome of REIP (Hunter, 2015), and *folA, folE, folKP* gene expression levels were detected in vitro by RT-qPCR assay (Bondar, 2015). Because of these findings, it is critical to quantify the folate levels to increase our knowledge of the nutritional interaction between the tick host and endosymbiotic bacteria.

Rickettsia monacensis pacifica in *Ixodes pacificus*

The characterization of novel rickettsia species was carried out using nucleotide sequences of a number of genes of *Rickettsia* species. For example, *16S rRNA*, citrate synthase gene (*gltA*), and surface-exposed antigenic protein genes (*ompA*, *ompB*, *sca4*, *17-kDa antigen*) (Fournier, 2003; Ishikura, 2003; Simser, 2002). We successfully propagated the REIP isolate using embryonic tick cell lines IRE11 and ISE6 (Simser, 2002; Munderlog, 1999), in complete L15B3100, a medium formulated for tick cell culture. Analysis of nucleotide sequences from complete opening frames of five genes, *ompA, ompB, 16S rRNA, gltA* and *sca4,* provided inference to the bacteria's classification among other *Rickettsia* species. The REIP isolate displayed 99.8%, 99.4%, 99.2%, 99.5% and 99.6% nucleotide sequence identity for *16S rRNA, gltA, ompA, ompB* and *sca4* gene, respectively, with genes of *R. monacensis* str. IrR/Munich, indicating the REIP isolate is a member of the *R. monacensis* complex. Phylogenetic analysis implied the REIP isolate is closely related to *R. buchneri* str. ISO7 and *R. monacensis* str. IrR/Munich, but is distinct from the rest of the spotted fever group rickettsiae. We propose the bacterium be named *Rickettsia monacensis* subsp. *pacifica* subsp. *nov.* To our knowledge, this is the first reported presence of *R. monacensis* in *I. pacificus* in North America.

Rickettsia monacensis pacifica is named to commemorate the tick host from which the bacterium was isolated, an obligate intracellular bacterium found within the western black legged tick, *I. pacificus*. The bacterium can be cultivated in tick cell lines IRE11 and ISE6 in medium formulated for tick cell culture at 26°C. The bacterium exhibits

morphology associated with the *Rickettsia* genus and the intracellular bacteria can be observed residing in the cytoplasm of Giemsa stained infected cells. The bacterium is susceptible to tetracycline and ciprofloxacin but is resistant to ampicillin (Walker, 1996; Alowaysi, 2015). The bacterium is an endosymbiont based on its nearly 100% prevalence in *I. pacificus* (Cheng, 2013a; Kurlovs, 2014). The pathogenicity of the bacterium remains to be determined.

Quantify Folate Concentration in *Rickettsia* infected tick cell lines

Folates are cofactors for biosynthetic enzymes in all eukaryotic and prokaryotic cells. Folate in their reduced tetrahydrofolate (THF) form are required as enzymatic cofactors in the folate cycle; a series of metabolic steps found in all cells (including both bacteria and animals) that is required for cell biosynthesis (Bailey and Gregory, 1999; Anderson, 2012). Most bacteria make folates *de novo*, previous research in Dr. Zhong's lab has demonstrated that all five folate biosynthesis genes exist in the genome of REIP (Hunter, 2015). Folate in cells have many different forms, but 5-methyltetrahydrofolate (5-MTHF) and 5-formyltetrahydrofolate (5-FTHF) are the active forms of folate (Kirsch, 2012; Obeid, 2013; Lakoff, 2014). So 5-MTHF and 5-FTHF were used as the standards to quantify the total folate level using HPLC-UV.

When HPLC-UV was performed, we first used 10mM ammonium acetate buffer for the mobile phase. Due to issues with clogging during our previous analysis (possibly due to protein precipitant or salt crystallization), we attempted to switch the mobile phase to a

0.1% formic acid buffer. The instrument called the Agilent 1050 Series was used in the beginning, but was later replaced by the Agilent 1200 Series. As for the column, the 150 x 2.1 mm Diamond Hydride (DH) column was initially used, but was later replaced by the 75 x 4.6 mm DH column. By adjusting the gradient method, we were able to improve the retention and separation of each compound within a reasonable time frame. Since our cooperators have had experience in detecting folate levels in food (Pesek, 2008, 2015), we initially followed their protocol in detecting folic acid levels in ISE6 and REIP infected cells. However, we were unable to find any folic acid peaks. Afterwards, we looked at the biologically active form of the folate found within the cell (e.g. 5-MTHF and 5-FTHF). We found that in all of the pellet samples there was an obvious peak within the 12.2-minute retention time, which happens to match the 5-MTHF standard retention time (Figure 21).

So far, we can only draw a conclusion that the folate concentration, specifically for 5-MTHF is significantly higher in the REIP infected cell pellet than the supernatant (with a p-value of 0.0043), and that the folate concentration in the REIP infected pellet is significantly higher than the ISE6 uninfected pellet sample (with the p-value 0.05). Based on the increased level of folate in the pellet sample, our data indicate that REIP is involved in the folate biosynthesis. However, we still do not have enough data to prove that *Rickettsia* is capable of *de novo* synthesis of folate, because the REIP infected starvation pellet sample is not statistically significant than the ISE6 uninfected pellet sample (with a p-value of 0.5). Analysis of the data revealed that the highest folate level was measured in the REIP-starvation-pellet sample. With a measured folate level of

0.6159 mg/L/10^6 cells in one of the three replicates. However, the second highest folate level from all the samples is the REIP pellet sample without starvation; this sample has a measured folate level of 0.4741 mg/L/10^6 cells. Compared with the supernatant samples, they are around 0.05 mg/L/10^6 cells. We also noticed that the fresh 5% FBS culture medium sample showed a high peak in supernatant sample comparison. Since the folate sample, especially for the active folate form, 5- MTHF, is sensitive to degradation. We believe the folate in the REIP-starvation pellet samples became degraded and pulled down the value of the average number. If this is true, then the experiments need to be repeated to prove our hypothesis. It is also difficult to measure peak area using HPLC software because of the low folate concentration in tick cell line. That HPLC software we use does not consider anything less than 5 mAUs/min (milli absorbance units) as significant. Because of this we have to generate the peak area manually, which may introduce human error. We have to generate the peak area by artificial, which will involve more human errors. To avoid this situation, we might load more samples in to HPLC machine, instead of using 10 uL. We sought to increase the initial sample amount, there is a bigger peak are showing in the end. However, it may bring the concern that the larger peak is not sharp enough, which indicate we need improve the methods to make different peak separate well.

Based on previous research in Dr. Zhong's lab, we only know REIP can produce tetrahydrofolate by dihydrofolate reductase (FolA) (Bodnar, 2015). However, it requires more steps to convert THF to 5-MTHF (Figure 3) (Rezk et al., 2003; Obeid et al., 2013). We found that the folate level in the uninfected ISE6 cells is lower than fresh L-15B300

complete culture medium, which confirms that ISE6 cells need to consume folate for their growth. This indicates that the excess folate level in the REIP infected sample should be synthesized by REIP.

Even though there is no sufficient data from this study to demonstrate that 5-MTHF is present within the samples, LC-MS/MS should be utilized to confirm its chemical identity of the candidate peak. In addition, the folate sample is easy to be degraded, especially for the active form 5-MTHF. Since Humboldt State University does not have the appropriate HPLC-UV or LC-MS/MS to run the tests, we had to bring our samples to San Jose State University and PHARMout Inc. (Sunnyvale, CA), where samples were measured to determine the folate concentrations by HPLC-UV and LC-MS/MS.

In the future, another test may be set in which an increase in incubation temperature will be used to inhibit REIP growth. This will allow us to compare the folate levels in high temperature samples with samples grown in optimal temperatures. Previously results have shown that REIP survives at 26 ºC, but they cannot survive and replicate at 34 ºC (data not shown). LC-MS/MS data is also required to confirm the identity of the substance at the 12.2 min peak as 5- MTHF.

In the end, we found that there is an observable peak showing at around the 9-minute mark in supernatant samples but is absent in the pellet samples, which may be caused by other folate derivatives. For example, *p*-aminobenzoic acid (PABA), dihydrofolic acid, etc. Knowing this we will include more folate derivatives as standards, this will allow us to gain a better understanding of the metabolic relationship between *Rickettsia* and ticks.

Mutant *folA* Gene in *Rickettsia*

To fill the knowledge gap of the nature symbiotic relationship between REIP and ticks, we believe the construction of the *folA* gene knockout mutant of REIP will help. Our lab has taken steps in constructing a *folA* gene knockout mutant of REIP. As we know, the *folA* gene is the last gene in the folate biosynthesis pathway (Zywnovan et al., 1997; Hunter, 2015). Bacteria can convert dihydrofolate to THF and release THF to the cell (Podnecky, 2017). This leads us to believe that inhibition of the REIP folate synthesis process can be done by manipulating the *folA* gene. We assume that if no THF produced from mutant REIP, the 5-MTHF levels should decrease in the mutated REIP-infected ISE6 cells. *pld, ompA sca4, rickA, rpoB* genes were manipulated in *Rickettsia* (Driskell, 2009; Noriea, 2015; Oliver, 2013; Rebecca, 2015). However, the manipulated genes in those studies were not essential genes for bacterial growth. We believe the construction of a *folA* gene (an essential gene) knockout mutant, while challenging, will provide us results that are more promising.

The TargeTron Gene Knockout system was used in constructing the *folA* gene knockout mutant, however throughout our efforts we have had to troubleshoot various problems. First, we tried different methods to avoid arcing during electroporation in order to improve transformation efficiency. Not only did we desalted the DNA sample, but also thoroughly washed the rickettsia with sucrose medium. We believe this will help in removing any leftover salts from the culture medium. Second, purification of REIP is needed prior to electroporation. The use of a 27-gauge needle combined with different

speeds centrifugation is not enough to purify REIP. As the 27-gauge needle lyses the host cell pellets, cell debris are formed. With a low speed centrifuge (275 x g), many bacteria are trapped and pelleted down with those cellular debris. Due to the small size of REIP, the cellular debris are easily recognized as real bacterium by mistake. The presence of cellular debris may be one of the reasons that the total number of REIP for electroporation cannot be reached. In addition, we do not recommend the use of more than 5 mL fully infected REIP-infected ISE6 cells, since too many cells can cause arcing during electroporation. Third, since the *folA* gene is an essential gene for the growth of bacteria, we added folinic acid to the complete L-15B300 medium as quick as possible after the electroporation. We were wondering if we could successfully get the *folA* knockout mutants of REIP, the mutant rickettsia may be dead or no growing. Compared with the wild type REIP, the *folA* knockout mutants cannot synthesize folate by themselves. They may not be able to compete with wild type in getting the low amount of folate present in the culture medium.

Therefore, instead of knocking out the folate gene, we will knock down the folate gene using Peptide Nucleic Acids (PNAs). PNAs are DNA mimics possessing a pseudopeptide backbone with conventional purine and pyrimidine bases (Nielsen et al., 1991). Antisense PNA molecules complementary to the Shine-Dalgarno or start codon region of mRNA effectively reduce translation (Good et al., 1998; Good et al., 1999). PNAs are designed to be complimentary with essential components such as ribosomal RNA demonstrating their use as effective microbial in a concentration dependent manner (Good et al., 1998), while offering the possibility of using PNA to study essential protein

function where a true knockout would preclude recovery of viable mutants. The ability of PNA to limit growth of facultative intracellular bacterium *Brucella suis* (Rajasekaran et al., 2013), implies the feasibility of using this strategy for reducing protein expression in obligate intracellular *Rickettsia* Spp. Designed PNA targeting mRNA for *rOmpB* from *R. typhi* and *rickA* from *R. montanesis* reduced the bacteria's ability to infect host cells (Pelc, et al., 2015).

The manipulation of the folate gene is challenging since folate is an essential for the bacterial growth. The results of this study may help in understanding the symbiotic relationship between REIP and *I. pacificus* ticks. Investigations into the endosymbiotic behavior of non-pathogenic species may lead to design more effective treatment methods to decrease the incidence of tick-borne diseases such as more specific anti-folate drugs or even the creation of transgenic ticks.

Measure Folate Level in Tick Sample

After measuring the folate level in REIP-infected ISE6 cells *ex vivo*, it is important to measure the folate level in tick samples. It may be difficult to detect the folate levels in ticks by using HPLC-UV because the number of rickettsiae in ticks is very low. However, we plan to measure the folate concentrations in ticks using LC-MS/MS, which has a higher sensitivity than the HPLC. Since the number of REIP is dramatically increased after the blood meal (Cheng, et. al. 2013a), we expect the engorged tick samples to have a higher concentration of folate than that in the flat ticks.

REFERENCES OR LITERATURE CITED

Aksoy S, (1995). Wigglesworthia gen. nov. and *Wigglesworthia glossinidia* sp. nov., taxa consisting of the mycetocyte-associated, primary endosymbionts of tsetse flies. *Int J Syst Bacteriol.* 45(4):848-51.

Alowaysi Maryam Tariq, (2015) Characterization of de novo folate biosynthesis of *Rickettsia* endosymbiont *Ixodes pacificus* in *Ixodes scapularis* ISE6 tick cell line. Humboldt state University.

Bailey, L. B., & Gregory, J. F. (1999). Folate metabolism and requirements. The Journal of nutrition, 129(4), 779-782.

Bekker, C. P., de Vos, S., Taoufik, A., Sparagano, O. A., & Jongejan, F. (2002). Simultaneous detection of Anaplasma and Ehrlichia species in ruminants and detection of Ehrlichiaruminantium in Amblyomma variegatum ticks by reverse line blot hybridization. *Veterinary microbiology*, *89*(2), 223-238.

Bell-Sakyi, L., Zweygarth, E., Blouin, E. F., Gould, E. A., & Jongejan, F. (2007). Tick cell lines: tools for tick and tick-borne disease research. *Trends in parasitology*, *23*(9), 450-457.

Bell-Sakyi L, Kohl A, Bente D A, et al. (2012). Tick cell lines for study of Crimean-Congo hemorrhagic fever virus and other arboviruses. Vector-Borne and Zoonotic Diseases, 12(9): 769-781.

Bodnar Jimmy, (2015) Biochemical characterization of the folate biosynthetic pathway of a rickettsial endosymbiont of *Ixodes pacificus*. Humboldt State University Library.

Brites-Neto, J., Duarte, K. M. R., & Martins, T. F. (2015). Tick-borne infections in human and animal population worldwide. *Veterinary world*, *8*(3), 301.

Blatch, S., Meyer, K. W., & Harrison, J. F. (2010). Effects of dietary folic acid level and symbiotic folate production on fitness and development in the fruit fly Drosophila melanogaster. *Fly*, *4*(4), 312-319.

Burkhardt, N. Y., Baldridge, G. D., Williamson, P. C., Billingsley, P. M., Heu, C. C., Felsheim, R. F., ... & Munderloh, U. G. (2011). Development of shuttle vectors for transformation of diverse *Rickettsia* species. PLoS One, 6(12), e29511.

CDC, Centers for Disease Control and Prevention, Centers for Disease Control and Prevention, 20 Apr. 2015, www.cdc.gov/ticks/life_cycle_and_hosts.html.

Chen, Y., McClane, B. A., Fisher, D. J., Rood, J. I., & Gupta, P. (2005). Construction of an alpha toxin gene knockout mutant of Clostridium perfringens type A by use of a mobile group II intron. *Applied and environmental microbiology*, *71*(11), 7542-7547.

Cheng, D., Lane,R. S., Moore, B. D. & Zhong, J. (2013a). Host blood meal dependent growth ensures transovarial transmission and transstadial passage of *Rickettsia* sp. Phylotype G021 in the western black-legged tick (*Ixodes pacificus*). *Ticks Tick Borne Dis* 4, 421-426.

Cheng, D., Vigil, K., Schanes, P., Brown R. N. & Zhong, J. (2013b). Prevalence and burden of two rickettsial phylotype (G021 and G022) in *Ixodes pacificus* from

California by real-time quantitative PCR. *Ticks Tick borne Dis* 4, 280-287.
Clover J R, Lane R S. (1993). Evidence implicating nymphal *Ixodes pacificus* (Acari: Ixodidae) in the epidemiology of Lyme disease in California. The American Journal of Tropical Medicine and Hygiene, 53(3): 237-240.
Cowdry E V. (1925). Studies on the etiology of heart water. Journal of Experimental Medicine, 42(2): 253-274.
Darby AC, Cho NH, Fuxelius HH, Westberg J, Andersson SG. (2007). Intracellular pathogens go extreme: genome evolution in the Rickettsiales. Trends Genet. 23(10):511-20.
de Crécy-Lagard, V., El Yacoubi, B., de la Garza, R. D., Noiriel, A., & Hanson, A. D. (2007). Comparative genomics of bacterial and plant folate synthesis and salvage: predictions and validations. *BMC genomics*, *8*(1), 245.
Dittrich S, Mitchell S L, Blagborough A M, et al. (2008). An atypical orthologue of 6-pyruvoyltetrahydropterin synthase can provide the missing link in the folate biosynthesis pathway of malaria parasites. Molecular microbiology, 67(3): 609-618.
Douglas AE, (2006). Phloem-sap feeding by animals: problems and solutions. *J Exp Bot.* 57(4):747-54.
Douglas, A. E. (2014). The molecular basis of bacterial–insect symbiosis. *Journal of molecular biology*, *426*(23), 3830-3837.
Driscool, (2017). Parasite of Eukaryotic Cells. MBio, vol. 8, no. 5, doi:10.1128/mbio.00859-17.
Driskell, L. O., Tucker, A. M., Woodard, A., Wood, R. R., & Wood, D. O. (2016). Fluorescence activated cell sorting of *Rickettsia prowazekii*-infected host cells based on bacterial burden and early detection of fluorescent rickettsial transformants. PloS one, 11(3), e0152365.
El Yacoubi B, Bonnett S, Anderson J N, et al. (2006). Discovery of a new prokaryotic type I GTP cyclohydrolase family. Journal of Biological Chemistry, 281(49): 37586-37593.
Felsheim, R. F., Herron, M. J., Nelson, C. M., Burkhardt, N. Y., Barbet, A. F., Kurtti, T. J., & Munderloh, U. G. (2006). Transformation of Anaplasma phagocytophilum. BMC biotechnology, 6(1), 42.
Fenech, M. (2012). Folate (vitamin B9) and vitamin B12 and their function in the maintenance of nuclear and mitochondrial genome integrity. *Mutation Research/Fundamental and Molecular Mechanisms of Mutagenesis*, *733*(1), 21-33.
Fermer, C., & Swedberg, G. (1997). Adaptation to sulfonamide resistance in Neisseria meningitidis may have required compensatory changes to retain enzyme function: kinetic analysis of dihydropteroate synthases from N. meningitidis expressed in a knockout mutant of Escherichia coli. *Journal of Bacteriology*, *179*(3), 831-837.
Foley, J. E., Nieto, N. C., Adjemian, J., Dabritz, H., & Brown, R. N. (2008). Anaplasma phagocytophilum infection in small mammal hosts of Ixodes ticks, western United States. *Emerging infectious diseases*, *14*(7), 1147.
Fournier, P. E., Dumler, J. S., Greub, G., Zhang, J., Wu, Y., & Raoult, D. (2003). Gene sequence-based criteria for identification of new *rickettsia* isolates and description

of *Rickettsia heilongjiangensis* sp. nov. Journal of clinical microbiology, 41(12), 5456-5465.

Fournier, P. E., & Raoult, D. (2007). Identification of rickettsial isolates at the species level using multi-spacer typing. BMC microbiology, 7(1), 72.

Fraser C, Hanage WP, Spratt BG. (2007). Recombination and the nature of bacterial speciation. Science. 315(5811):476-80.

Frazier, C. L., San Filippo, J., Lambowitz, A. M., & Mills, D. A. (2003). Genetic manipulation of *Lactococcus lactis* by using targeted group II introns: generation of stable insertions without selection. Applied and environmental microbiology, 69(2), 1121-1128.

Gengenbacher, M., Xu, T., Niyomrattanakit, P., Spraggon, G., & Dick, T. (2008). Biochemical and structural characterization of the putative dihydropteroate synthase ortholog Rv1207 of Mycobacterium tuberculosis. FEMS microbiology letters, 287(1), 128-135.

Gouy, M., Guindon, S., & Gascuel, O. (2009). SeaView version 4: a multiplatform graphical user interface for sequence alignment and phylogenetic tree building. Molecular biology and evolution, 27(2), 221-224.

Grochowski L L, Xu H, Leung K, et al. 2007) Characterization of an Fe2+-dependent archaeal-specific GTP cyclohydrolase, MptA, from *Methanocaldococcus jannaschii*. Biochemistry, 46(22): 6658-6667.

Hellmuth, C., Koletzko, B., & Peissner, W. (2011). Aqueous normal phase chromatography improves quantification and qualification of homocysteine, cysteine and methionine by liquid chromatography–tandem mass spectrometry. *Journal of Chromatography B*, *879*(1), 83-89.

Hornok, S., Mulvihill, M., Szőke, K., Gönczi, E., Sulyok, K. M., Gyuranecz, M., & Hofmann-Lehmann, R. (2017). Impact of a freeway on the dispersal of ticks and Ixodes ricinus-borne pathogens: forested resting areas may become Lyme disease hotspots. *Acta Veterinaria Hungarica*, *65*(2), 242-252.

Hossain T, Rosenberg I, Selhub J, et al. (2014). Enhancement of folates in plants through metabolic engineering. Proceedings of the National Academy of Sciences of the United States of America, 101(14): 5158-5163.

Indiragandhi, P., Anandham, R., Madhaiyan, M., Poonguzhali, S., Kim, G. H., Saravanan, V. S., & Sa, T. (2007). Cultivable bacteria associated with larval gut of prothiofos-resistant, prothiofos-susceptible and field-caught populations of diamondback moth, Plutella xylostella and their potential for, antagonism towards entomopathogenic fungi and host insect nutrition. *Journal of applied microbiology*, *103*(6), 2664-2675.

Karberg, K. A., Olsen, G. J., & Davis, J. J. (2011). Similarity of genes horizontally acquired by *Escherichia coli* and *Salmonella enterica* is evidence of a supraspecies pangenome. Proceedings of the National Academy of Sciences, 108(50), 20154-20159.

Kuehn, B. M. (2013). CDC estimates 300 000 US cases of Lyme disease annually. *Jama*, *310*(11), 1110-1110.

Kurlovs, A. H., Li, J., Cheng, D., & Zhong, J. (2014). Ixodes pacificus ticks maintain embryogenesis and egg hatching after antibiotic treatment of Rickettsia endosymbiont. *PloS one*, *9*(8), e104815.

Kurtti, T. J., Felsheim, R. F., Mattila, J. T., Baldridge, G. D., Burkhardt, N. Y., & Munderloh, U. G. (2006, March). Stable transformation of a tick (Ixodes scapularis) cell line with the Sleeping Beauty transposon system. In *IN VITRO CELLULAR & DEVELOPMENTAL BIOLOGY-ANIMAL* (Vol. 42, pp. 32A-32A). 514 DANIELS STREET, STE 411, RALEIGH, NC 27605 USA: SOCIETY IN VITRO BIOLOGY.

Kirsch SH, Herrmann W, Geisel J, Obeid R. (2012). Assay of whole blood (6S)-5-CH(3)-H(4) folate using ultra performance liquid chromatography tandem mass spectrometry. Anal Bioanal Chem. 404:895–902

Lakoff, A., Fazili, Z., Aufreiter, S., Pfeiffer, C. M., Connolly, B., Gregory, J. F., ... & O'Connor, D. L. (2014). Folate is absorbed across the human colon: evidence by using enteric-coated caplets containing 13C-labeled [6S]-5-formyltetrahydrofolate. *The American journal of clinical nutrition*, *100*(5), 1278-1286.

Lambowitz, A. M., & Zimmerly, S. (2004). Mobile group II introns. Annu. Rev. Genet., 38, 1-35.

Lucock M, Daskalakis J. (2000). New perspectives on folate status: a differential role for the vitamin in cardiovascular disease, birth defects and other conditions [J]. British journal of biomedical science, 57(3): 254.

Simser, J. A., Palmer, A. T., Fingerle, V., Wilske, B., Kurtti, T. J., & Munderloh, U. G. (2002). Rickettsia monacensis sp. nov., a spotted fever group Rickettsia, from ticks (Ixodes ricinus) collected in a European city park. *Applied and Environmental Microbiology*, *68*(9), 4559-4566.

Margulis Lynn, (1967). "On the origin of mitosing cells". J Theor Biol. 14 (3): 255–274

McCutcheon J P, Moran N A. (2010). Functional convergence in reduced genomes of bacterial symbionts spanning 200 My of evolution. Genome biology and evolution, 2: 708-718.

McClure, E. E., Chávez, A. S. O., Shaw, D. K., Carlyon, J. A., Ganta, R. R., Noh, S. M., ... & McBride, J. W. (2017). Engineering of obligate intracellular bacteria: progress, challenges and paradigms. *Nature Reviews Microbiology*, *15*(9), nrmicro-2017.

Mereschkowsky, Konstantin. (1910). Theorie der zwei Plasmaarten als Grundlage der Symbiogenesis, einer neuen Lehre von der Ent-stehung der Organismen. Biol Centralbl. 30: 353-367.

Merhej V, Angelakis E, Socolovschi C, Raoult D. (2014). Genotyping, evolution and epidemiological findings of *Rickettsia* species. Infect Genet Evol 25:122-137.

Moran NA, McCutcheon JP, Nakabachi AL. (2008). Genomics and evolution of heritable bacterial symbionts. Annu Rev Genet. 42:165-90.

Munderloh, U. G., & Kurtti, T. J. (1989). Formulation of medium for tick cell culture. Experimental and Applied Acarology, 7(3), 219-229.

Munderloh, U. G., Liu, Y., Wang, M., Chen, C., & Kurtti, T. J. (1994). Establishment,

maintenance and description of cell lines from the tick Ixodes scapularis. *The Journal of parasitology*, 533-543.

Munderloh, U. G., Tate, C. M., Lynch, M. J., Howerth, E. W., Kurtti, T. J., & Davidson, W. R. (2003). Isolation of an Anaplasma sp. organism from white-tailed deer by tick cell culture. *Journal of clinical microbiology*, *41*(9), 4328-4335.

Noda H, Munderloh U G, Kurtti T J. (1997). Endosymbionts of ticks and their relationship to Wolbachia spp. and tick-borne pathogens of humans and animals. Applied and environmental microbiology, 63(10): 3926-3932.

Noriea, N. F., Clark, T. R., & Hackstadt, T. (2015). Targeted knockout of the *Rickettsia rickettsii* OmpA surface antigen does not diminish virulence in a mammalian model system. MBio, 6(2), e00323-15.

Nuttall P A, Labuda M. (2003). Dynamics of infection in tick vectors and at the tick–host interface [J]. Advances in virus research, 60: 233-272.

Obeid, R., Holzgreve, W., & Pietrzik, K. (2013). Is 5-methyltetrahydrofolate an alternative to folic acid for the prevention of neural tube defects?. *Journal of perinatal medicine*, *41*(5), 469-483.

O'Connor, T. J., Adepoju, Y., Boyd, D., & Isberg, R. R. (2011). Minimization of the *Legionella pneumophila* genome reveals chromosomal regions involved in host range expansion. Proceedings of the National Academy of Sciences, 108(36), 14733-14740.

Oliver, J. D., Burkhardt, N. Y., Felsheim, R. F., Kurtti, T. J., & Munderloh, U. G. (2014). Motility characteristics are altered for Rickettsia bellii transformed to overexpress a heterologous rickA gene. *Applied and environmental microbiology*, *80*(3), 1170-1176.

Oliver, J. D., Chávez, A. S. O., Felsheim, R. F., Kurtti, T. J., & Munderloh, U. G. (2015). An Ixodes scapularis cell line with a predominantly neuron-like phenotype. *Experimental and Applied Acarology*, *66*(3), 427-442.

Padgett K A, Lane R S. (2001). Life cycle of *Ixodes pacificus* (Acari: Ixodidae): timing of developmental processes under field and laboratory conditions. Journal of Medical Entomology, 38(5): 684-693.

Pelc, R. S., McClure, J. C., Kaur, S. J., Sears, K. T., Rahman, M. S., & Ceraul, S. M. (2015). Disrupting protein expression with peptide nucleic acids reduces infection by obligate intracellular *Rickettsia*. PloS one, 10(3), e0119283.

Pesek, J. Matyska, M. T. (2007). A Comparison of Two Separation Modes: HILIC and Aqueous Normal Phase Chromatography. *LCGC North America*, *25*, 480.

Pesek, J. J., Matyska, M. T., Fischer, S. M., & Sana, T. R. (2008). Analysis of hydrophilic metabolites by high-performance liquid chromatography–mass spectrometry using a silica hydride-based stationary phase. *Journal of chromatography A*, *1204*(1), 48-55.

Pesek, J. J and Matyska. (2015). Aqueous Normal Phase Chromatography Using Silica Hydride-Based Stationary Phases. Advances in Liquid Chromatography: New Developments in Stationary Phases and Supports for Drugs and Bioanalytical Applications, pp. 20–31., doi:10.4155/fseb2013.14.99.

Perronne, C. (2014). Lyme and associated tick-borne diseases: global challenges in the context of a public health threat. *Frontiers in cellular and infection microbiology*, *4*.

Perutka, J., Wang, W., Goerlitz, D., & Lambowitz, A. M. (2004). Use of computer-designed group II introns to disrupt Escherichia coli DExH/D-box protein and DNA helicase genes. *Journal of molecular biology*, *336*(2), 421-439.

Piesman, J., Clark, K. L., Dolan, M. C., Happ, C. M., & Burkot, T. R. (1999). Geographic survey of vector ticks (Ixodes scapularis and Ixodes pacificus) for infection with the Lyme disease spirochete, Borrelia burgdorferi. *Journal of vector ecology: journal of the Society for Vector Ecology*, *24*(1), 91-98.

Polo, G., Acosta, C. M., Labruna, M. B., & Ferreira, F. (2017). Transmission dynamics and control of Rickettsia rickettsii in populations of Hydrochoerus hydrochaeris and Amblyomma sculptum. *PLOS Neglected Tropical Diseases*, *11*(6), e0005613.

Podnecky, N. L., Rhodes, K. A., Mima, T., Drew, H. R., Chirakul, S., Wuthiekanun, V., ... & Schweizer, H. P. (2017). Mechanisms of resistance to folate pathway inhibitors in Burkholderia pseudomallei: deviation from the norm. *MBio*, *8*(5), e01357-17.

Pyne C, Bognar A L. (1992). Replacement of the *folC* gene, encoding folylpolyglutamate synthetase-dihydrofolate synthetase in *Escherichia coli*, with genes mutagenized in vitro. Journal of bacteriology, 174(6): 1750-1759.

Pribat, A., Jeanguenin, L., Lara-Núñez, A., Ziemak, M. J., Hyde, J. E., de Crécy-Lagard, V., & Hanson, A. D. (2009). 6-pyruvoyltetrahydropterin synthase paralogs replace the folate synthesis enzyme dihydroneopterin aldolase in diverse bacteria. *Journal of bacteriology*, *191*(13), 4158-4165.

Radulovic, S., Troyer, J. M., Beier, M. S., Lau, A. O., & Azad, A. F. (1999). Identification and molecular analysis of the gene encoding *Rickettsia typhi* hemolysin. Infection and immunity, 67(11), 6104-6108.

Rachek L. I, Tucker AM, Winkler HH, Wood DO. (1998).Transformation of *Rickettsia prowazekii* to rifampin resistance. J Bacteriol. 180(8):2118-24.

Rachek, L. I., Hines, A., Tucker, A. M., Winkler, H. H., & Wood, D. O. (2000). Transformation of *Rickettsia prowazekii* to erythromycin resistance encoded by the *Escherichia coli ereB* gene. Journal of bacteriology, 182(11), 3289-3291.

Rajasekaran, P., Alexander, J. C., Seleem, M. N., Jain, N., Sriranganathan, N., Wattam, A. R & Boyle, S. M. (2013). Peptide nucleic acids inhibit growth of *Brucella suis* in pure culture and in infected murine macrophages. International journal of antimicrobial agents, 41(4), 358-362.

Raoult, D., FOURNIER, P. E., Eremeeva, M., Graves, S., Kelly, P. J., Oteo, J. A., ... & Zhang, L. (2005). Naming of rickettsiae and rickettsial diseases. *Annals of the New York Academy of Sciences*, *1063*(1), 1-12.

Renesto, P., Gouin, E., & Raoult, D. (2002). Expression of green fluorescent protein in *Rickettsia conorii*. Microbial pathogenesis, 33(1), 17-21.

Rezk, B. M., Haenen, G. R., van der Vijgh, W. J., & Bast, A. (2003). Tetrahydrofolate and 5-methyltetrahydrofolate are folates with high antioxidant activity. Identification of the antioxidant pharmacophore. *FEBS letters*, *555*(3), 601-605.

Riley, S. P., Macaluso, K. R., & Martinez, J. J. (2015). Electrotransformation and clonal isolation of Rickettsia species. *Current protocols in microbiology*, 3A-6.

Rizzoli A, Silaghi C, Obiegala A, Rudolf I, Hubalek Z, Foldvari G, Plantard O, Vayssier-Taussat M, Bonnet S, Spitalska E, Kazimirova M. (2014). *Ixodes ricinus* and Its Transmitted Pathogens in Urban and Peri-Urban Areas in Europe: New Hazards and Relevance for Public Health. Front Public Health 2:251.

Rossi M, Amaretti A, Raimondi S. (2011). Folate production by probiotic bacteria. Nutrients 3:118-134.

Rothacher L, Ferrer, Suay M, Vorburger C. (2016). Bacterial endosymbionts protect aphids in the field and alter parasitoid community composition. Ecology, 97(7): 1712-1723.

Sahni, S. K., Narra, H. P., Sahni, A., & Walker, D. H. (2013). Recent molecular insights into rickettsial pathogenesis and immunity. *Future microbiology*, *8*(10), 1265-1288.

Saitou, N., & Nei, M. (1987). The neighbor-joining method: a new method for reconstructing phylogenetic trees. Molecular biology and evolution, 4(4), 406-425.

Sakurai, M., Koga, R., Tsuchida, T., Meng, X. Y., & Fukatsu, T. (2005). *Rickettsia* symbiont in the pea aphid *Acyrthosiphon pisum*: novel cellular tropism, effect on host fitness, and interaction with the essential symbiont Buchnera. Applied and environmental microbiology, 71(7), 4069-4075.

Schroeder, C. L., Narra, H. P., Rojas, M., Sahni, A., Patel, J., Khanipov, K & Sahni, S. K. (2015). Bacterial small RNAs in the Genus Rickettsia. BMC genomics, 16(1), 1075.

Socolovschi, Cristina, et al. (2013). Tick-Borne Spotted Fever Rickettsioses." Hunter's Tropical Medicine and Emerging Infectious Disease, pp. 546–552., doi:10.1016/b978-1-4160-4390-4.00064-3.

Spreadbury, J. (2013). Folic Acid and Its Receptors.

Snyder, A. K., & Rio, R. V. (2015). "Wigglesworthia morsitans" Folate (Vitamin B9) Biosynthesis Contributes to Tsetse Host Fitness. *Applied and environmental microbiology*, *81*(16), 5375-5386.

Silva, M. T. (2012). Classical labeling of bacterial pathogens according to their lifestyle in the host: inconsistencies and alternatives. *Frontiers in microbiology*, *3*.

Simser, J. A., Palmer, A. T., Fingerle, V., Wilske, B., Kurtti, T. J., & Munderloh, U. G. (2002). Rickettsia monacensis sp. nov., a spotted fever group Rickettsia, from ticks (Ixodes ricinus) collected in a European city park. *Applied and Environmental Microbiology*, *68*(9), 4559-4566.

Sonenshine. E. Daniel. (1993). Biology of tick #1.

Sybesma W, Burgess C, Starrenburg M, et al. (2004). Multivitamin production in *Lactococcus lactis* using metabolic engineering. Metabolic engineering, 6(2): 109-115.

Taylor M, Mediannikov O, Raoult D, Greub G. (2012). Endosymbiotic bacteria associated with nematodes, ticks and amoebae. FEMS Immunol Med Microbiol 64:21-31.

Tsuchida T, Koga R, Horikawa M, et al. (2010). Symbiotic bacterium modifies aphid body color. Science, 330(6007): 1102-1104.

Viklund J, Ettema TJG, Andersson SGE, (2012). Independent genome reduction and phylogenetic reclassification of the oceanic SAR11 clade. Mol Biol Evol 29: 599–615

Wang, H., Zhao, P., Liang, X., Gong, X., Song, T., Niu, R., & Chang, J. (2010). Folate-PEG coated cationic modified chitosan–cholesterol liposomes for tumor-targeted drug delivery. Biomaterials, 31(14), 4129-4138.

Walker H David. (1996). Medical Microbiology 4th edition. Chapter 38. The University of Texas Medical Branch at Galveston.

Walker TS, (1984). Rickettsial interactions with human endothelial cells in vitro: adherence and entry. *Infect Immun.* 44(2):205-10.

Wegkamp, A., van Oorschot, W., de Vos, W. M., & Smid, E. J. (2007). Characterization of the role of para-aminobenzoic acid biosynthesis in folate production by Lactococcus lactis. *Applied and environmental microbiology*, *73*(8), 2673-2681.

Werren J H, O'Neill S L. (1997). The evolution of heritable symbionts. Influential passengers: inherited microorganisms and arthropod reproduction, 1-41.

Wernegreen J J, Funk D J. (2004). Mutation exposed: a neutral explanation for extreme base composition of an endosymbiont genome. Journal of molecular evolution, 59(6): 849-858.

Wheeler P R. (1992). One-carbon requirements of Mycobacterium leprae: need for the folate pathway. International journal of leprosy and other mycobacterial diseases, 60: 445-445.

Winkler HH, (1985). Early events in the interaction of the obligate intracytoplasmic parasite, *Rickettsia prowazekii*, with eukaryotic cells: entry and lysis. Ann Inst Pasteur Microbiol. 1986 May-Jun; 137A (3):333-6.

Winkler HH. (1990). *Rickettsia* species (as organisms), Annu Rev Microbiol. 44:131-53

Yao, J., Zhong, J., Fang, Y., Geisinger, E., Novick, R. P., & Lambowitz, A. M. (2006). Use of targetrons to disrupt essential and nonessential genes in Staphylococcus aureus reveals temperature sensitivity of Ll. LtrB group II intron splicing. *Rna*, *12*(7), 1271-1281.

Yunker C E, Kuttler K L, Johnson L W. (1987). Attenuation of *Babesia bovis* by in vitro cultivation.Veterinary parasitology, 24(1-2): 7-13.

Zhu, Y., Fournier, P. E., Eremeeva, M., & Raoult, D. (2005). Proposal to create subspecies of *Rickettsia conorii* based on multi-locus sequence typing and an emended description of *Rickettsia conorii*. BMC microbiology, 5(1), 11.

Znazen, A., Hammami, A., Bouattour, A., Marrekchi, C., Lahiani, D., Khrouf, F & M'Ghirbi, Y. (2013). Multispacer typing of *Rickettsia* isolates from humans and ticks in Tunisia revealing new genotypes. Parasites & vectors, 6(1), 367.

Zywno-van Ginkel, S., Dooley, T. P., Suling, W. J., & Barrow, W. W. (1997). Identification and cloning of the Mycobacterium avium fol A gene, required for dihydrofolate reductase activity. *FEMS microbiology letters*, *156*(1), 69-78.

APPENDIX A

Appendix A: PCR reaction primers, annealing temperatures, and amplicon sizes for identify *Rickettsia* species. *16S rRNA*, *gltA*, *ompA dksA-xerC*, *mppA-purC*, and *rpmE-tRNA^{fMet}*, *β-actin* were used.

Gene name	**Primer (5'-3')**	**Annealing Temperature**	**Amplicon size (bp)**	**Reference**
16S rRNA	F-AGAGTTTGATCCTGGCTCAG R-AACGTCATTATCTTCCTTGC	58°C	436	Simser et al., 2002
gltA	F-GGGGGCCTGCTCACGGCGG R-ATTGCAAAAAGTACAGTGAACA	50°C	382	Simser et al., 2002
ompA	F-ATGGCGAATATTTCTCCAAAAA R-AGTGCAGCATTCGCTCCCCCT	60 °C	530	Simser et al., 2002
dksA-xerC	F-TTTTCATGACGCTCTTGAGC R-GTAAAGAAAGAATAATTCCGTGGTT	58°C	165	Fournier and Raoult, 2007
mppA-purC	F-GCATATGCRGTRGGTAGTTAT R-CACACGCCCAAATTCTAATT	59 °C	1000	Raoult, 2007
rpmE-tRNA^{fMe}	F-TTCCGGAAATGTAGTAAATCAATC R-TCAGGTTATGAG CCTGACGA	57 °C	368	Raoult, 2007
β-actin	F-TTGTCCGCGACATCAAGGA R-CGGGAAGCTCGTAGGACTTCT	57 °C	110	Cheng *et al*., 2013

APPENDIX B

Appendix B: Gene names and GenBank sequence accession numbers used in this study

Strains for MLST	16S rRNA	*gltA*	*ompA*	*ompB*	*sca4*
R. aeschlimannii	NZ_CCER01000003	HM050276	U83446	HM050278	HM050275
R. africae str. ESF-5	CP001612	CP001612	CP001612	CP001612	CP001612
R. akari str. Hartford	CP000847	CP000847	CP000847	CP000847	CP000847
R. asiatica str. IO1	NR041840	AB297811	NA	DQ110870	DQ110869
R. australis str. Cutlack	CP003338	CP003338	CP003338	CP003338	CP003338
R. bellii str. RML369 C	CP000087	CP000087	NA	CP000087	CP000087
R. buchneri str. ISO7	JFKF01000109	JFKF01000076	JFKF01000169	JFKF01000150	JFKF01000160
R. conorii str. Malish 7	AE006914	AE006914	AE006914	AE006914	AE006914
R. felis str. URRWXCal2	CP000053	CP000053	CP000053	CP000053	CP000053
R. heilongjiangensis str. 054	CP002912	CP002912	CP002912	CP002912	CP002912
R. helvetica str. C9P9	L36212	KP866150	NA	KP866151	AF163009
R. honei str. RB	NR025967	U59726	AF018076	AF123711	DQ309095
R. japonica str. YH	AP011533	AP011533	AP011533	AP011533	AP011533
R. massiliae str. MTU5	CP000683	CP000683	CP000683	CP000683	CP000683
R. monacensis str. IrR/Munich	LN794217	LN794217	LN794217	LN794217	LN794217
R. montanensis subsp. *pacifica* IPO1	NZ_LAOP01000001	KJW02430	KJW02278	KJW03404	KJW03052

Strains for MLST	16S rRNA	*gltA*	*ompA*	*ompB*	*sca4*
R. montanensis str. OSU 85-930	CP003340	CP003340	CP003340	CP003340	CP003340
R. parkeri str. Portsmouth	CP003341	CP003341	CP003341	CP003341	CP003341
R. peacockii str. Rustic	CP001227	CP001227	CP001227	CP001227	CP001227
R. philipii str. 364D	CP003308	CP003308	CP003308	CP003308	CP003308
R. prowazekii str. BuV67-CWPP	CP003393	CP003393	NA	CP003393	CP003393
R. raoultii str. Khabarovsk	CP010969	CP010969	CP010969	CP010969	CP010969
R. rhipicephali str. 3-7-female6-CWPP	CP003342	CP003342	CP003342	CP003342	CP003342
R. rickettsii str. Hlp2	CP003311	CP003311	CP003311	CP003311	CP003311
R. sibirica subsp. mongolitimonae	NZ AHZB01000018	NZ_AABW01000001	U83439	DQ097083	DQ097084
R. slovaca str. D-CWPP	CP003375	CP003375	CP003375	CP003375	CP003375
R. tamurae str. AT1	NR042727	NZ_CCMG01000011	NA	DQ113910	DQ113911
R. typhi str. B9991CWPP	CP003398	CP003398	NA	CP003398	CP003398

Strains for MST	*dksA-xerC* intergenic spacer	*mppA-purC* intergenic spacer	*rpmE-tRNA-fMet* intergenic spacer
R. aeschlimanniistr. MC16T	DQ008272	DQ008293	DQ008255
R. africae str. ESF-5	AY820037	DQ008301	DQ008246
R. akari str. MK	AY820045	DQ008291	DQ008260
R. asiatica	EF123265	NA	EF123269
R. australis str. Phillips	DQ008273	DQ008294	DQ008259

Strains for MST	*dksA-xerC* intergenic spacer	*mppA-purC* intergenic spacer	*rpmE-tRNA-fMet* intergenic spacer
R. bellii	DQ008282	NA	DQ852359
R. buchneri str. ISO7	CM000770	CM000770	CM000770
R. conorii subsp. israelensis	KF539825	KF539832	KF539829
R. felis str. URRWXCal2	DQ008281	DQ008302	DQ008258
R. heilongjiangensis str. 054	EF123264	EF123267	EF123268
R. helvetica str. C9P9	DQ008275	DQ008296	DQ648586
R. honei str. TT118	DQ008276	DQ008297	DQ008252
R. japonica str. YM	DQ008277	DQ008298	DQ008253
R. massiliae str. Mtut1T	DQ008267	DQ008288	DQ008256
R. monacensis str. IrR/Munich	LN794217	LN794217	LN794217
R. montanensis subsp. *pacifica* IPO1	KX505844	KX505842	KX505843
R. montanensis str. M/5-6	AY820021	DQ008300	DQ008254
R. parkeri str. Portsmouth	DQ008266	DQ008287	DQ008249
R. peacockii	NA	NA	NA
R. philipii	NA	NA	NA
R. prowazekii str. Madrid E	DQ008269	DQ008290	AY695447
R. raoultii str. Khabarovsk	EF140690	EF140692	EF140694
R. rhipicephali str. 3-7-female6-CWPP	AY820044	DQ008289	DQ008257
R. rickettsii str. R	AY820038	DQ008286	DQ008250
R. sibirica subsp. mongolitimonae	DQ008263	DQ008284	DQ008248
R. slovaca str. 13B	DQ008278	DQ008299	DQ008251

Strains for MST	*dksA-xerC* intergenic spacer	*mppA-purC* intergenic spacer	*rpmE-tRNA-fMet* intergenic spacer
R. tamurae	EF123266	NA	EF123270
R. typhi str. Wilmington	DQ008271	DQ008292	DQ008261

APPENDIX C

Appendix C. Cell death ratio of ISE6 cell line after starvation treatment.

Hours	Alive	Dead	Total Cell count	Death ration
0	386	147	533	0.27579
1	285	192	477	0.40252
2	333	320	653	0.49005
4	275	318	593	0.53626
6	196	241	437	0.55149
8	184	307	491	0.62525
9	187	364	551	0.66062
12	154	309	463	0.66739

APPENDIX D

Appendix D. Cell counting and cell death ratio for ISE6 uninfected cells, REIP cell and REIP starvation cell before HPLC sample pre-treatment.

Sample	Total	Dead	Cell viability
ISE6-1	14	0	
	45	1	0.966101695
ISE6-2	59	2	
	30	1	0.97752809
ISE6-3	31	1	
	24	0	0.979166667
REIP-1	31	0	
	59	2	0.977777778
REIP-2	156	5	
	162	6	0.965408805
REIP-3	146	3	
	154	2	0.983333333
REIP-1-starvation	218	7	
	274	18	0.949186992

Sample	Total	Dead	Cell viability
REIP-2-starvarvation	175	9	
	224	14	0.94235589
REIP-3-starvation	308	17	
	171	8	0.947807933
ISE6-starvation	164	18	0.896226415

APPENDIX E

Appendix E. Averaged folate level and standard deviation for each sample. 0% and 5% FBS means L-15B300 medium with added 0% FBS and 5% FBS. ISE6-starvation-pellet sample, 0% FBS and 5% FBS only detect once, no Standard deviation data available.

Sample Name	Averaged	SD
ISE6-S	0.039321229	0.068105146
ISE6-P	0.058023338	0.052833988
REIP-S	0.002877681	0.004982887
REIP-P	0.251395265	0.19292144
REIP-Starv-S	0.042227762	0.073139634
REIP-Starv-P	0.22547137	0.338749423
ISE6-Starv-P	0.0219761	
0% FBS	0.062853757	
5% FBS	0.285981899	

APPENDIX F

Appendix F. Nucleotide sequences obtained from Elim biopharma Inc were aligned by Codoncode Aligner. The random nucleotide sequences labeled as “N” in the pARR plasmid intron are aligned with the *folA* specific primer sequences in the intron clones of 182 and 474.

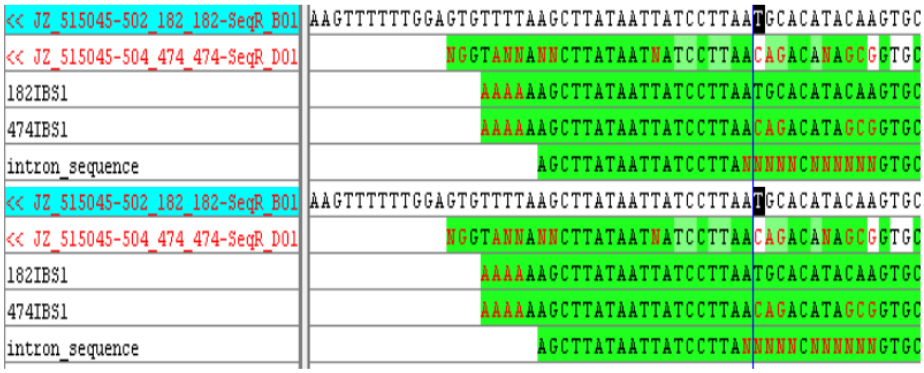

APPENDIX G

Appendix G. Original intron sequence. The “N” sites underline are replaced with designed primer sequence nucleotide.

AGCTTATAATTATCCTTANNNNNCNNNNNNGTGCGCCCAGATAGGGTGTTAA
GTCAAGTAGTTTAAGGTACTACTCTGTAAGATAACACAGAAAACAGCCAACC
TAACCGAAAAGCGAAAGCTGATACGGGAACAGAGCACGGTTGGAAAGCGAT
GAGTTACCTAAAGACAATCGGGTACGACTGAGTCGCAATGTTAATCAGATAT
AAGGTATAAGTTGTGTTTACTGAACGCAAGTTTCTAATTTCGNTTNNNNNNCG
ATAGAGGAAAGTGTCTGAAACCTCTAGTACAAAGAAAGGTAAGTTANNNNN
NNNGACTTATCTGTTATCACCACATTTGTACAATCTG